Evolution of prudent predation in complex food webs: mechanism and evidence

Orestes U. Gutierrez Al-Khudhairy[1] and Axel G. Rossberg[1*]

Running title: Prudent predation in complex food webs

for consideration as Ecology Letters "Perspective"

May 4, 2021

[1] School of Biological and Chemical Sciences, Queen Mary University of London, Mile End Road, London, E1 4NS, United Kingdom

[*] Corresponding Author (++44-75-5139-6243, a.rossberg@qmul.ac.uk)

Keywords: evolution of cooperation, invasive alien species, spawner-recruitment relations, biogeography, functional responses, apparent competition, allometric scaling, trophic interaction strength, ecological modelling, analytic theory

180	words in abstract
7567	words in main text
430	words in Box 1
125	words in Box 2
6	figures
2	tables
2	text boxes
135	references

Author contributions OUGAK and AGR jointly conceived the study, conceived and developed the metapopulation model, and wrote the manuscript. OUGAK conceived and implemented the deconstructed model formulation and the simplified model for consumer impact, compiled evidence on invasive alien, and performed model simulations and statistical analyses. AGR developed the analytic theory, implemented the full model formulation and compiled most evidence from the empirical literature.

Abstract

Prudent predators catch sufficient prey to sustain their populations but not as much as to undermine their populations' survival. The idea that predators evolve to be prudent has been dismissed in the 1970s, but the blunt arguments invoked then are untenable in light of modern evolution theory. Evolution of prudent predation has repeatedly been demonstrated in two-species predator-prey metacommunity models. However, the vigorous population fluctuations that these models predict are not widely observed. Here we show that in complex model food-webs prudent predation evolves by a different mechanism. We make testable predictions for empirical signatures of this mechanism and its outcomes. Then we discuss how these predictions are borne out across freshwater, marine, and terrestrial ecosystems. Demonstrating explanatory power of evolved prudent predation well beyond the question of predator-prey coexistence, the predicted signatures explain unexpected declines of invasive alien species, the shape of stock-recruitment relations of fish, and the clearance rates of pelagic consumers across the latitudinal gradient and 15 orders of magnitude in body mass. Specific research to further test and mobilise the utility of this theory is proposed.

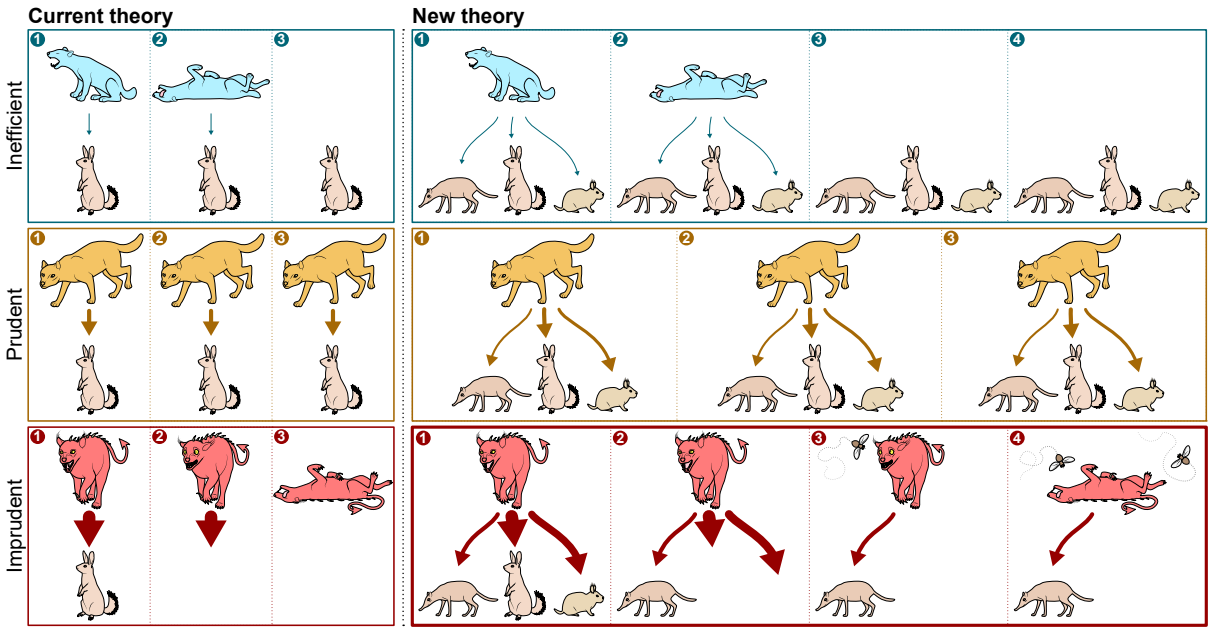

Figure 1: **Comparison of current and new theories of selection for prudent predation.** Arrows point from consumer to resource, arrow width indicates attack rate. According to both theories, consumers that are either too inefficient (top row) or imprudently aggressive—approaching Darwinian Daemons (bottom row), easily get extirpated. Prudent consumers (middle row) persist for longer. Contrasting the prevailing theory, our model predicts that imprudent consumers feeding on multiple resources "hang on" after extirpating their most important resources, feeding on less suitable resources that persist. This, however, leaves them in a weak position. Any subsequent change in community structure, e.g., spread of a disease (symbolised by flies), can push them over the edge, leading to extirpation. The resulting separation of the ultimate and the proximate cause of extirpation, seen similarly for invasive alien consumers, is a signature of the new theory. Illustration: Rebecca Gelernter/Near Bird Studios

1 Introduction

Altruism, the display of traits that are detrimental to the fitness of individuals but benefit others (Nowak, 2012), is observed throughout the living world, including plants (Dudley, 2015), non-human mammals (Schino & Aureli, 2010) and bacteria (Refardt *et al.*, 2013). Controversial, however, remains whether it also occurs in the most relentless kind of ecological interaction, foraging on living resources. We shall call consumers (species feeding on living resources, e.g. predators, herbivores) *prudent* (Slobodkin, 1960) if they feed at a rate sufficient to sustain their populations but not so much that resource overexploitation would become detrimental to their populations' persistence (Fig. 1). We will speak of *evolved prudence* (or similar) when prudence arises through the consumer's adaptation to its native resource community by mutation and selection.

The idea that consumers have evolved to be prudent was been proposed by Slobodkin (1960) based on observations that the ecological efficiencies of laboratory populations of *Daphnia* and *Artemia* nauplii (Slobodkin, 1964) that were experimentally harvested such as to maximise long-term biomass yield was numerically close to the efficiencies calculated by Lindeman (1942) and others form field observations. Slobodkin was soon criticised on the basis that evolution of prudence required group selection, and that

the conditions for group selection to operate were not typically satisfied in nature (Maynard Smith & Slatkin, 1973). Meanwhile, however, evolution of prudent predation has repeatedly been demonstrated in two-species consumer-resource metacommunity models (Fig. 1, left; Gilpin, 1975; Haraguchi & Sasaki, 2000; Pels *et al.*, 2002; Rauch *et al.*, 2003; Messinger & Ostling, 2013), including individual-base models (Rand *et al.*, 1995; Mitteldorf *et al.*, 2002; Goodnight *et al.*, 2008). This deserves repeating: prudent predation easily evolves in metacommunity models. The sceptics' intuition that prudent predation can hardly evolve *because it requires group selection* is false.

Moreover, it has become clear that the very distinction between "kin selection" (which has more sympathy in the scientific community) and "group selection" is not fundamentally one between processes but one between mathematical methods (Lion *et al.*, 2011). For problems where both methods are applicable, they yield the exact same result (Jansen, 2011). A categorical dismissal of evolved prudent predation is therefore now more difficult—Slobodkin's (2009) own later doubts notwithstanding.

Furthermore, there is another, more profound issue indicating the need for some form of adaptation of consumer-resource interaction strengths, which has puzzled ecologists since Nicholson (1933) and Gause (1934): getting consumer and resource to coexist in simple model systems, both experimental and mathematical, requires careful adjustment of parameters. In the classical consumer-resource model of Rosenzweig & MacArthur (1963), for example, consumer-resource oscillations set in at values of attack rate a that are only $(1+\tau^{-1})$-times larger than the value of a required for the consumer to eat enough to survive, with τ denoting the proportion of time consumers spend at population-dynamical equilibrium "handling" resources rather then "searching for" them in the behavioural model underlying the Type II functional response (Holling, 1959). With typical parameters, the range of oscillation-free coexistence therefore spans just an order of magnitude or so in a. Beyond this range, population minima reached by the resource during oscillations decline exponentially with a, soon leading to extinction of any finite resource population—and subsequent extinction of the consumer. In multi-resource models, the range in attack rates separating invadibility of consumers and extinction of resource through consumer-mediated (or "apparent" *sensu* Holt, 1977) competition is similarly constrained (Rossberg, 2013, Sec. 15.3). In general, the relevant dimensionless parameter is the product of assimilation efficiency, attack rate and resource carrying capacity (both in biomass units) divided by the consumer's rate of biomass loss due to respiration and mortality (below *respiration+mortality* rate). To permit co-existence, it must lie between one and some tight, model-dependent upper limit. To assume that in nature this condition is regularly satisfied by pure chance would be implausible. Considering the large variety of known consumer strategies to locate, chase, trap and/or subdue resources, of resource strategies to hide, escape, and defend themselves, and of typical resource abundances, variation in the parameter over much more than two orders of magnitude would be expected. How then can consumers and resource coexist in the wild?

This problem has been intensely discussed amongst theorists during the 1970s, but without satisfactory resolution (Slatkin & Maynard Smith, 1979). Next to invocation of some form of altruism, two other important lines of thought were developed. Exploring the first, Schaffer & Rosenzweig (1978) evaluated the joint evolutionary dynamics of consumer and resource in the Rosenzweig-MacArthur model, to see under which conditions an evolutionary stable steady state with stable consumer-resource coexistence is reached. They found this to be possible when, measured on the relevant scale, the resource evolves faster than the consumer. Slobodkin (1974) had come to that same conclusion on intuitive grounds. He argued, less convincingly, that this condition should be satisfied because predators are torn between adaptation to a variety of different defence strategies by different prey (e.g. running *vs.* hiding), which results in slower adaptation to any particular defence, while prey stick with a single defence strategy. Another argument why consumers should evolve slower than their resource is the "Life-Dinner Principle" (Dawkins & Krebs, 1979): for the resource it is about survival, for the consumer just a meal. The evidence, however, is to the contrary: studies of food-web topologies, in conjunction with phylogenetic data (Bersier & Kehrli, 2008; Eklöf & Stouffer, 2016) or on their own (Rossberg *et al.*, 2006), consistently show that in a joint niche space in which consumer traits need to match resource traits to yield maximum attack rate (Rossberg *et al.*, 2010), resources tend to evolve much slower than consumers.

The second line of thought considers structured population models. Stage-structured population models (Maynard Smith & Slatkin, 1973; Slobodkin, 1974) can mitigate the problem of overexploitation, but do not appear to ultimately resolve it (Slatkin & Maynard Smith, 1979). More promising are spatially structured models (Hilborn, 1975; Hastings, 1977). In agreement with early intuition (Nicholson, 1933; Nicholson & Bailey, 1935) and experiments pioneered by Huffaker (1958) and Pimentel *et al.* (1963), repeated recolonisation can permit metapopulations of consumers and resources to coexist even when consumers locally extirpate their resources. However, while this mechanism relaxes constraints on parameters for coexistence, it does not entirely eliminate them. Consumers still go extinct if their attack rates are too high or too low for a given dispersal rate (Mitteldorf *et al.*, 2002) or their dispersal rates too high or too low for a given attack rate (Hilborn, 1975). Furthermore, if one permits the consumer's attack rate to evolve in such models—and why not—it naturally adjusts itself at values permitting coexistence (Gilpin, 1975; Mitteldorf *et al.*, 2002). Similar trends have been observed in experiments (Pimentel *et al.*, 1963). Such metacommunity models therefore also hardly serve as alternatives to evolved prudence in explaining consumer-resource co-existence.

Yet, scepticism about these metacommunity models of one consumer and one resource species, i.e., with *monophagous* consumers is justified—with or without evolution of attack rate. The scenarios of local booms and busts or vigorous population oscillations they predict might describe pests raging across landscapes, but are not sufficiently common to support them as general explanations for consumer-resource coexistence in nature (Maynard Smith & Slatkin, 1973; Taylor, 1990). Detailed empirical reports of such

repeated boom-bust cycles for closely associated consumer-resource pairs present them as ecological curiosities rather than a generic phenomenon (Dempster, 1971; Eber & Brandl, 1994; Schöps, 2002; Johst & Schöps, 2003, further examples reviewed by Taylor 1991).

This mismatch between predicted and observed phenomenology, not the perceived problem of group selection, should be the main reason for scepticism about evolved prudence. And persistent scepticism is evident, e.g., from recent proposals to compute attack rates from fundamental physical and physiological constraints (Pawar *et al.*, 2012; Ho *et al.*, 2019; Portalier *et al.*, 2019; Hirt *et al.*, 2020) and in the role that assumed physiological trade-offs or pleiotropy—indirectly constraining attack rates—continue to play in evolutionary models of consumer-resource interactions (van Velzen & Gaedke, 2017; Schreiber *et al.*, 2018; Fleischer *et al.*, 2018).

A clue for resolving this mismatch in phenomenology comes from noting that, in a review by Roy & Chattopadhyay (2007) on the closely related "paradox of enrichment" (Rosenzweig, 1971), all cited experiments in which enrichment (i.e. increased resource carrying capacity) led to stronger oscillations used only one resource species, while all those where this was not observed involved multiple resources (excluding Kirk (1998), who artificially stabilised resource abundance). Instead of inducing oscillations, enrichment led to replacement of more suitable by less suitable resources (Persson *et al.*, 2001).

Here we show that a similar process can lead to selection for prudence (Fig. 1, bottom right) and overcome the mismatch between the predicted and observed phenomenology of its evolution. This requires taking into account that most consumers are *polyphagous*, feeding on multiple resource, and are parts of complex ecological communities that continuously turn over in species composition (Dornelas *et al.*, 2014; Yoccoz *et al.*, 2018; O'Sullivan *et al.*, 2020). The resulting evolutionary mechanism (Fig. 1, right) does not depend on predator-prey oscillations (Rosenzweig, 1971) and aligns better with observations.

Early studies demonstrating evolution of prudence in food webs employed a model (the PDMM, Rossberg *et al.*, 2008; Rossberg, 2013, Sec. 22.3) that characterises species by body size and other evolving traits, which in turn jointly determine interactions and interaction strengths. Communities assembled by this model share key properties with marine food-webs (Fung *et al.*, 2015). Feeding follows Type II functional responses with prey switching (van Leeuwen *et al.*, 2013; Morozov & Petrovskii, 2013), which can lead to both stable population-dynamical equilibria (Fung *et al.*, 2015) and complex oscillatory dynamics (Rossberg *et al.*, 2008). The insight that prudence can evolve in such a detailed, realistic model is important—but many of these details are inessential. In simple two-layer food-web models with linear functional responses, studied since MacArthur (1969), the same phenomenon is observed (Rossberg, 2013, Sec. 20.4). Using such a model, we address three questions:

1. By what mechanism does prudence evolve in food-web assembly models?

2. What kind of observations would provide evidence that this mechanism is active in nature?

3. To what extent has this evidence been observed?

2 The two-level Lotka-Volterra food-web assembly model and its deconstruction

2.1 The full model

Our working model is a Lotka-Volterra-type model in which S_C consumers forage on a community of S_R living resources:

$$\frac{\mathrm{d}\hat{B}_j^\mathrm{R}}{\mathrm{d}t} = \left[s\left(1 - \frac{\hat{B}_j^\mathrm{R}}{K}\right) - \sum_{k=1}^{S_\mathrm{C}} a_{jk}\hat{B}_k^\mathrm{C} \right] \hat{B}_j^\mathrm{R} \qquad (1 \le j \le S_\mathrm{R}), \tag{1a}$$

$$\frac{\mathrm{d}\hat{B}_k^\mathrm{C}}{\mathrm{d}t} = \left[\epsilon \sum_{j=1}^{S_\mathrm{R}} a_{jk}\hat{B}_j^\mathrm{R} - \rho_k \right] \hat{B}_k^\mathrm{C} \qquad (1 \le k \le S_\mathrm{C}). \tag{1b}$$

Here t is time, $\hat{B}_j^\mathrm{R}$ is the time-dependent population biomass (or biomass density) of the j-th resource, and $\hat{B}_k^\mathrm{C}$ that of the k-th consumer. For simplicity, we assume identical intrinsic growth rates s and carrying capacities K of resources, absence of direct competition between producers, and identical assimilation efficiencies ϵ for all consumers. The coefficient $a_{jk} \ge 0$ represents the attack rate of consumer k on resource j. Finally, ρ_k denotes the respiration+mortality rate (dimension 1/Time) of consumer k. In most cases, we assume identical $\rho_k = \rho$ for all consumers.

To simplify analytic calculations, we express attack rates by the dimensionless coefficients $H_{jk} = \alpha_{0k} a_{jk}$, with $\alpha_{0k} = \epsilon K/\rho_k$ (abbreviated to α_0 if all $\rho_k = \rho$), and measure resource biomass B_j^R in units of K and consumer biomass B_k^C in units of $\alpha_{0k} s$ (Tab. 1), yielding the equivalent system

$$\frac{\mathrm{d}B_j^\mathrm{R}}{\mathrm{d}t} = s\left[1 - B_j^\mathrm{R} - \sum_{k=1}^{S_\mathrm{C}} H_{jk} B_k^\mathrm{C} \right] B_j^\mathrm{R} \qquad (1 \le j \le S_\mathrm{R}), \tag{2a}$$

$$\frac{\mathrm{d}B_k^\mathrm{C}}{\mathrm{d}t} = \rho_k \left[\sum_{j=1}^{S_\mathrm{R}} H_{jk} B_j^\mathrm{R} - 1 \right] B_k^\mathrm{C} \qquad (1 \le k \le S_\mathrm{C}). \tag{2b}$$

Model communities are assembled through iterative invasion of random species (Post & Pimm, 1983; Caldarelli *et al.*, 1998). At each iteration, it is first decided at random, with equal probability, whether the newly invading species will be a consumer or a resource. Candidate species of the chosen type are then sampled at random as described below until one is found that can invade the community (i.e. for which the term in brackets in Eq. (2) is positive). After adding this species to the community with an initial biomass of M_min, population dynamics are simulated until a new equilibrium is reached. Species whose populations fall below M_min are removed as extirpated.

Note that, for resources j in equilibrium that are not fed upon, $B_j^\mathrm{R} = 1$. Hence, by Eq. (2b), a

consumer k has population growth rate $\rho_k \left[\sum_{j=1}^{S_\mathrm{R}} H_{jk} - 1\right]$ if it does not share resources with other consumers and its own abundances B_k^C is too low to affect its resource populations. This becomes $\sum_{j=1}^{S_\mathrm{R}} H_{jk} - 1$ when measuring growth rate in units of ρ_k. In this expression, the sum $\sum_{j=1}^{S_\mathrm{R}} H_{jk} = \epsilon K \rho_k^{-1} \sum_{j=1}^{S_\mathrm{R}} a_{jk}$ corresponds to the dimensionless quantity identified as being constrained by prudence in Introduction. Indeed, defining $R_k = \sum_{j=1}^{S_\mathrm{R}} H_{jk}$, the classical invadibility criterion (Grainger *et al.*, 2019) implies that $R_k > 1$ is necessary for consumer-resource co-existence, and below we show that much larger R_k are detrimental.

Traditional community models have often been formulated in terms of numerical population sizes rather then population biomasses. We would recover such a formulation here, e.g., by assuming that all individuals of species k have the same body mass m_k and disregarding the contribution of respiration to ρ_k. Then R_k becomes the basic reproduction number (often denoted "R_0") of consumer k: the mean lifetime number of offspring at low consumer abundance and in absence of interspecific competition (reviewed by Lion & Metz, 2018). Since in the general case R_k plays an analogous role, we call R_k the *basic reproduction number* here.

2.2 Sampling of new species

In Appendix S1 (in Supporting Information) we motivate the following scheme for sampling the traits and interactions of newly invading species in our model. Each consumer k is associated with a so-called *base attack rate* trait a_k that scales attack rates a_{jk}. When a new consumer k is sampled, its base attack rate is chose as

$$a_k = \gamma_0 \gamma_1^{\xi} a_r, \tag{3}$$

where r is one of the S_C resident consumers, sampled at random, ξ is a standard normally distributed random number (both sampled anew for each candidate consumer), and the two parameters $\gamma_0 > 0$ and $\gamma_1 > 1$ control bias (*sensu* Pomiankowski *et al.*, 1991) and size, respectively, of what we will call "mutations" of base attack rate in the model. We choose $\gamma_0 < 1$ to represent degeneration of traits under insufficient selection. For our choices of model parameter (Tab. 1), about 20% of "mutations" raise attack rate ($a_k > a_r$), which is plenty in view of observed distributions of fitness effects of mutations (Eyre-Walker & Keightley, 2007; Castellano *et al.*, 2019). This scheme to sample "mutants" is justified by an assumption that the distribution of base attack rates within the focal community is representative of the implicit metacommunity from which species invade.

The attack rates a_{jk} for newly invading consumers k or resources j are then sampled from log-normal distributions scaled by a_k, i.e.,

$$a_{jk} = a_k e^{\sigma \xi_{jk}} \quad \text{or} \quad H_{jk} = \alpha_0 a_{jk} = \alpha_0 a_k e^{\sigma \xi_{jk}}, \tag{4}$$

Table 1: List of symbols and model parameters

Symbol	Description	Value
A	Resident's growth rate term	$R_l - 1$
a, a_k	Base attack rate (of consumer k)	Eq. (3)
a_{jk}	Rate of attack rate of resource j by consumer k	$a_k e^{\sigma\xi_{jk}}$
α_{0k}	Attack rate scaling factor	$K\epsilon\rho_k^{-1}$
B	Resident l's intraspecific competition term	$\sum_j H_{jl}^2$
$\hat{B}_j^{\mathrm{R}}$	Resource biomass (density) in physical units	KB_j^{R}
$\hat{B}_k^{\mathrm{C}}$	Consumer biomass (density) in physical units	$\alpha_{0k} s B_k^{\mathrm{C}}$
B_j^{R}	Dimensionless resource biomass	
B_k^{C}	Dimensionless consumer biomass	
β	Abundance scaling factor in birth probability formula	0.45
C	Focal species's growth rate term	$R_k - 1$
C_{m}	Maintenance food concentration	$\rho_k/(\epsilon a_{jk})$
D	Interspecific competition term	$\sum_j H_{jk}H_{jl}$
ϵ	Assimilation efficiency	0.1
γ_0	Mutation bias of base attack rate	$0.8^{1/2}$
γ_1	Mutational variation of base attack rate	$1.3^{1/2}$
H_{jk}	Dimensionless attack rate of resource j by consumer k	$\alpha_{0k}a_{jk}$
K	Resource carrying capacity in absence of consumers	1
L, $L(a)$	Mean duration of species persistence in community	
$M_{\min}$	Dimensionless biomass extirpation threshold	10^{-5}
$P_{\mathrm{inv}}(a)$	Invasion probability	
$\rho = \rho_k$	Rate of consumer biomass loss by respiration and mortality	0.1
R, $R(a)$	Lifetime mean number of "offspring" *populations*	
R_k	Basic reproduction number of *individuals* of species k	$\sum_j H_{jk}$
s	Resource intrinsic per capita growth rate	1
S_{C}	Consumer species richness	
S_{R}	Resource species richness	
SSB	Fish population standing stock biomass	
Rec	Fish population recruitment rate	
σ	Standard deviation of log attack rates	4
t	Time	
ξ, ξ_{jk}	Standard normal random variates	$\mathcal{N}(0,1)$

with independent standard-normally distributed ξ_{jk} ($1 \leq j \leq S_{\mathrm{R}}$). These log-normal distributions can be understood as resulting from trait matching between random consumers and resources in a high-dimensional trophic niche space (Appendix S1). The spread σ of the log-normal distribution is a measure of consumer specialisation (Rossberg *et al.*, 2011) and kept fixed throughout the simulations.

Using Eqs. (3) and (4), we avoid setting an inherent scale for attack rates. The magnitude of attack rates is controlled by a_k, and evolution of a_k according to Eq. (3) is scale free: it is invariant under multiplication of all a_k, a_r by a constant factor. Below we show that the evolutionary stable magnitude of a_k is ultimately determined at the ecosystem level.

2.3 The deconstructed model formulation

To gain a better understanding of the processes operating during community assembly and turnover, we developed a novel *deconstructed formulation* of this model. Population dynamics are broken up into a sequence of phases that permit approximate analytic descriptions, thus avoiding simulation of the

system of ODEs (2). In Box 1, we named these in analogy to phases of ecological invasions (without claiming identity), as distinguished and discussed by Lockwood *et al.* (2013) and Reise *et al.* (2006). The analogies become clearest when interpreting our model as describing an island community that is occasionally colonised by species from other islands.

Contrasting Law & Morton (1996), our deconstructed formulation does not aim to reproduce the dynamics of the full model in all detail, just its system-level phenomenology. For this, surprisingly coarse approximations are sufficient. These build on the observation that only few resources tend to contribute sizably to a consumer's diet (Rossberg *et al.*, 2011; Rossberg, 2013, Ch. 12), which we reproduce by our choice of model parameters (Tab. 1, see Rossberg, 2013, Chs. 11, 12 for detailed discussion). This justifies the simplifying assumption that at most one other consumer needs to be considered to determine a consumer's persistence with a given set of resources. The full algorithm is described in Box 1. Its formulation highlights the role of the *main resource* of a consumer k, defined as that extant resource for which H_{jk} is largest over all j.

2.4 Model steady states

We compared simulations of full and deconstructed formulations with the same set of parameters (Tab. 1). As shown in Fig. 2a,b, the richness of consumers (S_C) and resources (S_R) reached in the steady state is similar for the two formulations, and so is the pattern of richness fluctuations.

In Fig. 2c,d we compare time series of community mean logarithmic base attack rates $\overline{\log_{10} a}$ for both formulations. The evolutionary steady state reached is independent of the a_k value of the seeding community of consumers (Fig. 2c,d), and differs only slightly between model formulations.

Accounting for the log-normal distribution of sampled attack rates, Eq. (4), steady state means reported in Fig. 2 imply that during establishment $R_k = \sum_j^{S_\mathrm{R}} H_{jk}$ is on average $\alpha_0 a_k e^{\sigma^2/2} S_\mathrm{R} \approx 17$ (full) and ≈ 7 (deconstructed). This is evolved prudent predation. Through the adaptation of base attack rates, basic reproduction numbers R_k have stabilised at values greater but not much greater than 1.

3 How prudence evolves in our model

To uncover how prudence evolves in our model, we explore three layers of depth of model analysis. These relate to the evolutionary forces at work, the effect of base attack rate on consumer competitiveness, and the restructuring of resource communities by consumers. These analyses are followed by summary and discussion of the full mechanism in a non-technical language.

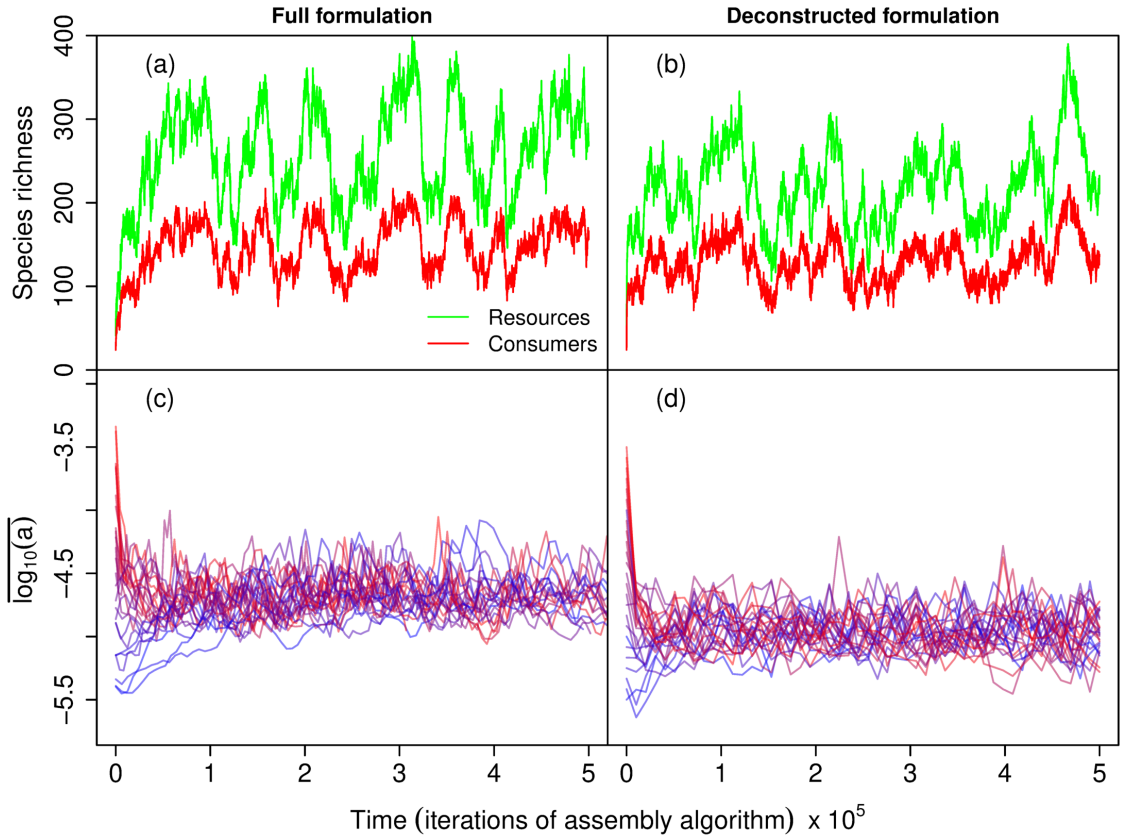

Figure 2: **Approaches of full and deconstructed model formulations to steady state.** The richness of resources S_{R} (green) and consumers S_{C} (red) reaches quasi-steady states (i.e. they fluctuate around a constant mean) for both full (a) and deconstructed (b) formulation. Furthermore, the quasi-steady states of both formulations display similar means and patterns of variation. Likewise, community mean base attack rates $\overline{\log_{10}(a)}$ reaches a quasi-steady states for both (c) full and (d) deconstructed formulation, with steady state values being independent of initial values (colour graduation). With the overline indicating averages, we obtain from the model steady state (between $2{\cdot}10^5$ - $5{\cdot}10^5$ iterations), $\overline{S}_{\mathrm{R}} = 260$, $\overline{S}_{\mathrm{C}} = 147$, $\overline{\log_{10} a} = -4.67$ (full), $\overline{S}_{\mathrm{R}} = 224$, $\overline{S}_{\mathrm{C}} = 125$, $\overline{\log_{10} a} = -4.96$ (deconstructed).

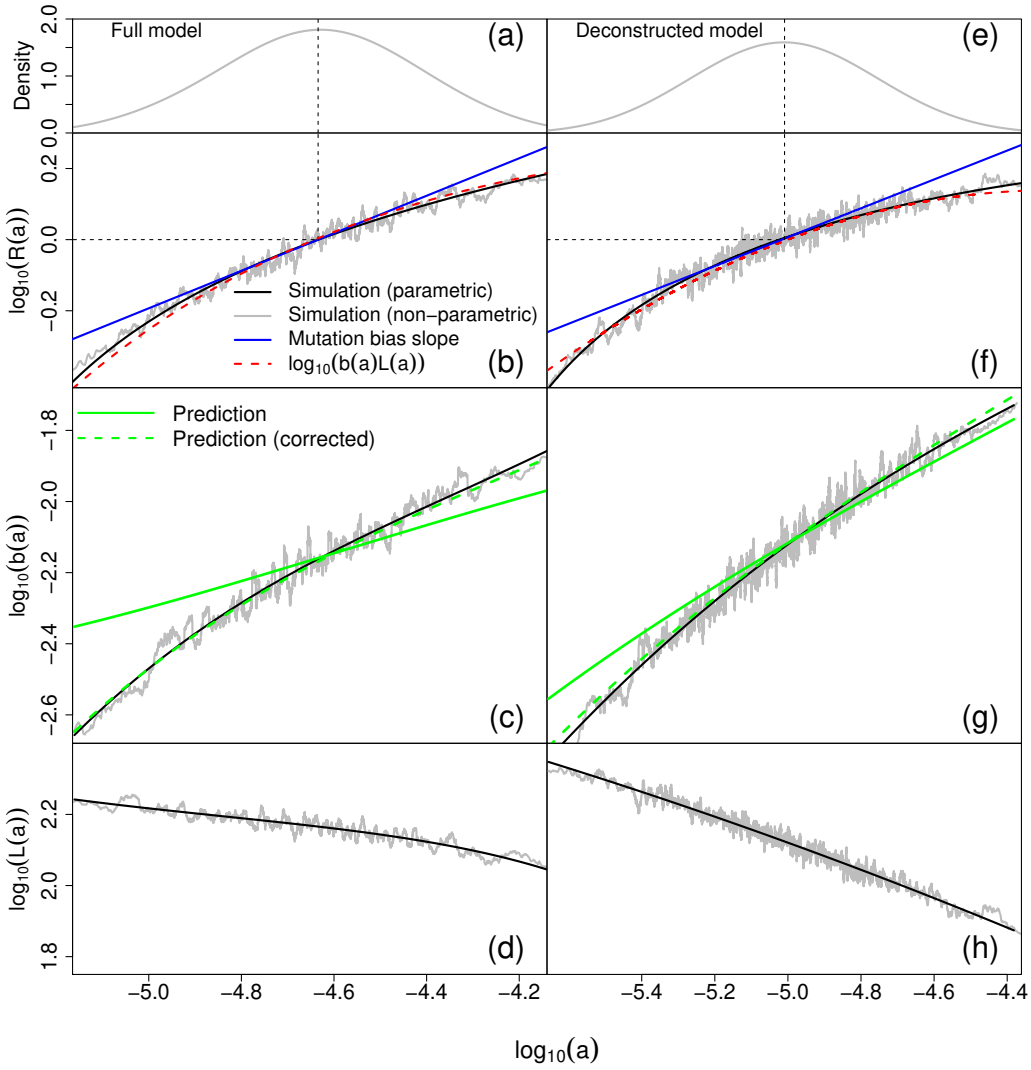

Figure 3: **Meta-community level fitness landscape.** Panels (a) and (e) display the distribution of logarithmic base attack rate ($\log_{10} a$) in simulations, with the dashed vertical line representing the simulation mean ($\log_{10} a^*$). Panels (b) and (f) represent mean logarithmic reproductive output ($\log_{10} R(a)$), which we use as a fitness proxy. The remaining panels display the decomposition of $\log_{10} R(a)$ into the additive contributions from logarithmic birth rate $\log_{10} b(a)$ (c), (g) and logarithmic mean lifetime $\log_{10} L(a)$(d), (h) according to Eq. (12). We obtained $b(a)$ and $L(a)$ from simulations and verified the decomposition in panels (b) and (f) (red dashed lines). Observe that the curve for $\log_{10} R(a)$ passes zero and is tangential to the predicted mutation bias slope at $a = a^*$, confirming our interpretation of $\log_{10} R(a)$ as a fitness proxy. Results for the for the full model [(a)-(e)], Eq. (2), are semi-quantitatively reproduced by the deconstructed formulation [(f)-(h)] (Sec. 2.3). All graphs are based on a single simulation with 5×10^5 iterations for each model formulation, initiated with base attack rates close to the steady state mean. The first 10^5 iterations were discarded as burn-ins. Curves in (a) and (e) are obtained using the `density` function of the R statistical software with standard parameters. The non-parametric curves in (b), (c), (d), (f), (g) and (h) were computed by taking rolling means of $R(a)$, $b(a)$, $L(a)$ for individual consumers and their $\log_{10} a$ values with a window size equivalent to 1% of the total sample size. The parametric curves are quadratic least-square fits to the rolling means on double-logarithmic axes. The predicted birth rates in (c) and (g) were calculated according to Eq. (S24), the mutation bias slop according to Eq. (11) (converting from natural to decimal logarithms).

Box 1 The deconstructed formulation of our community assembly model. Conditions (5)-(9) are derived in Appendix S2.

1. Initialise the model community with a small set of randomly sampled consumers and resources ($S_\mathrm{C} = 10$ and $S_\mathrm{R} = 20$). The subsequent addition of species, resulting in community assembly and turnover, occurs by:
2. **Transport (i):** Sample with equal probability whether the next species to invade is a consumer or a resource.
3. If a consumer is to invade:
   (a) **Transport (ii):** Sample the base attack rate and interaction coefficients H_{jk} for a candidate invader k as described in Sec. 2.2.
   (b) **Establishment:** Test whether this consumer can invade using first the criterion that the consumer should satisfy the **invadability criterion**

$$\sum_j^{S_\mathrm{R}} H_{jk} - 1 > 0 \tag{5}$$

   as a minimum requirement for consumer k to persist, and then the (stronger but computationally more expensive) requirement that it should not get extirpated through **exploitative competition** from each of the resident consumers l according to

$$\sum_j^{S_\mathrm{R}} H_{jk} - 1 < \left(\sum_j^{S_\mathrm{R}} H_{jk}H_{jl}\right) \frac{\sum_j^{S_\mathrm{R}} H_{jl} - 1}{\sum_j^{S_\mathrm{R}} H_{jl}^2}. \tag{6}$$

   If consumer k cannot invade, repeat from Step 3a until a consumer is sampled that can.
   (c) **Spread (within community):** Remove all of the invading consumer's resources j that get **overexploited** during consumer k's early boom phase, which happens when

$$H_{jk} > -\log\left(M_\mathrm{min}\right). \tag{7}$$

   (d) **Bust after boom:** If the invading consumer now fails the invadibility criterion, Eq. (5), remove it and continue with Step 5.
   (e) **Impact (resource serial extirpations):** If

$$\sum_j^{S_\mathrm{R}} H_{jk} - 1 > \frac{\sum_j^{S_\mathrm{R}} H_{jk}^2}{\max_j(H_{jk})}, \tag{8}$$

   indicating the extirpation of j's main resource though **consumer-mediated ("apparent") competition**, remove that resource and repeat Step 3e.
4. If a resource is to invade:
   (a) **Transport (ii):** Sample the resource's interaction coefficients H_{jk} as described in Sec. 2.2 and add it to the community.
   (b) **Expansion & Impact:** While there are consumers satisfying the condition for consumer mediated resource extirpation, Eq. (8), repeat the following:
      i. Chose one of these consumers at random and call it l.
      ii. Remove l's main resource.
      iii. Remove any consumers k that now fail to satisfy the invadibility criterion, Eq. (5).
5. **Adjustment (exploitative competition):** Test which consumers k satisfy the condition for exploitative competitive exclusion, Eq. (6), by any other consumers l. Then remove all that do.
6. **Adjustment (Pyrrhic competition):** Test which consumers k satisfy the condition for loss in Pyrrhic competition, Eq. (9) below, against any other consumers l. Then remove *the main resource* of each k that does.
7. **Adjustment (starvation)**: Remove all consumers that now fail the invadibility criterion, Eq. (5).
8. Repeat from Step 2 for a predetermined number of iterations.

In Step 6 **Phyrric competition** between consumers k and l ($k \neq l$) leads to extirpation of k's main resource i if:

$$\left(\sum_j^{S_\mathrm{R}} H_{jk}^2\right)\left(\sum_j^{S_\mathrm{R}} H_{jl}^2\right) - \left(\sum_j^{S_\mathrm{R}} H_{jk}H_{jl}\right)^2 < \left(\sum_j^{S_\mathrm{R}} H_{jk} - 1\right)\left(H_{ik}\sum_j^{S_\mathrm{R}} H_{jl}^2 - H_{il}\sum_j^{S_\mathrm{R}} H_{jk}H_{jl}\right) + \left(\sum_j^{S_\mathrm{R}} H_{jl} - 1\right)\left(H_{il}\sum_j^{S_\mathrm{R}} H_{jk}^2 - H_{ik}\sum_j^{S_\mathrm{R}} H_{jk}H_{jl}\right) \tag{9}$$

N.B.: In Appendix S2 we provide a simple algorithmic formulation of this condition.

3.1 Evolutionary forces

To understand the evolutionary forces leading to prudent predation, we first reconstruct the relevant fitness landscape. Note that while we speak here of consumer species or populations as if these were units of selection, the precise formulation would be that the units of selection in our model are consumer individuals invading communities to form new resident populations. As common in theories for evolution of virulence of infectious diseases (see also Sec. 3.6), our theory does not describe the details of consumer evolution within communities (for diseases: pathogens within hosts). Because each community is different, such short-term adaptation is unlikely to have much bearing on the long-term evolution of base attack rates (Appendix S1).

The approximate normal distribution of logarithmic base attack rates ($\ln a$) in the model steady state (Figs. 3a,e) suggests an analysis in terms of $\ln a$. We therefore reformulate our model for inheritance of

base attack rates, Eq. (3), as:

$$\ln a_k = \ln \gamma_0 + \xi \ln \gamma_1 + \ln a_r. \tag{10}$$

Hence $\ln \gamma_0$ represents the size of the mutation bias and $(\ln \gamma_1)^2$ the mutational variance of $\ln a$.

We define $R(a)$ as the mean number of populations that inherit their base attack rates *via* Eq. (3) from a given population with base attack rate a (the "mean lifetime reproductive success" of *populations*). Denoting by a^* the geometric mean of a and by $\mathrm{var}(\ln a)$ the variance of $\ln a$ in the evolutionary steady state, we derive in Appendix S3 the evolutionary steady state condition

$$\left.\frac{d \ln R(a)}{d \ln a}\right|_{a=a^*} \approx -\frac{\ln \gamma_0}{\mathrm{var}(\ln a)}. \tag{11}$$

It describes a balance between a fitness gradient (left-hand-side) and the counteracting effect of mutation bias (right-hand-side). We verify this relation graphically in Fig. 3b and f. As expected, for both the full and the deconstructed model (i) the equilibrium condition for species richness, $\ln R(a^*) = 0$ (i.e., $R(a^*) = 1$), holds, and (ii) the straight line with slope $-\ln \gamma_0 / \mathrm{var}(\ln a)$ is tangential to the graph of $\ln R(a)$ against $\ln a$ at $a = a^*$, as predicted by Eq. (11). This confirms $R(a)$ as a suitable fitness proxy.

We proceed by disentangling the mechanisms determining $R(a)$. Define $L(a)$ as the mean time populations with base attack rate a remain in the community, and $b(a)$ as the mean rate at which they generate new invaders. We can factorise $R(a) = b(a)L(a)$ because the ancestors of candidates for consumer invasion are chosen randomly with equal probability in our model, implying that the rate at which a species with base attack rate a gives rise to a new invasion is independent of the lifetime of this species. Hence

$$\ln R(a) = \ln b(a) + \ln L(a). \tag{12}$$

In Figs. 3c,d,g,h (black lines) we show these two additive components of $\ln R(a)$ for both model formulations, as determined numerically from the model steady states.

The "birth" rate $b(a)$ exhibits the increasing trend with base attack rate a that one would naively expect. In fact, the curve can be understood at an analytic level. We included in Figs. 3c,g two analytic approximations of $b(a)$. The first is based on a log-normal approximation for the distribution of the sum $\sum_{j=1}^{S_\mathrm{R}} H_{jk}$ in the invadibility criterion, Eq. (5). The full calculation, taking into account the mutation bias and the fact that we measure time in units of consumer invasions, is presented in Appendix S4. The resulting dependence of $b(a)$ on $\ln a$ has the functional form of a cumulative normal distribution. The second approximation accounts for competition between consumers by multiplying the sum above with a fitting parameter β, which represents an average mean scaled biomass of resources encountered by invading consumers. With $\beta = 0.25$ (full) and $\beta = 0.45$ (deconstructed), this reproduces the form of

$b(a)$ found in our model (Fig. 3c,g). This analytic model implies that the graph of $\ln b(a)$ *vs* $\ln a$ always has a positive slope, is bending downwards, and reaches a plateau for large $\ln a$. In the following, we explain why, somewhat counter-intuitively, the mean population "lifetime" $L(a)$ declines with increasing base attack rate a.

3.2 How base attack rate affects consumer competitiveness

The deconstructed formulation separates different ecological processes with a clarity not offered by simulations of the full model, permitting us to gain insights into the mechanisms controlling population "lifetime" in the model. We consider it justified to rely on the deconstructed formulation for this, because it reproduces the full formulation's phenomenology well (Figs. 2, 3).

Because around 96% of consumer extirpations are triggered either by the competitive exclusion condition, Eq. (6), or by failure of the invadability condition, Eq. (5), which implies the former, and because this does not depend much on the base attack rate of the extirpated species (Fig. S4), we focus here on the drivers of competitive exclusion.

The deconstructed formulation's condition for competitive exclusion of a consumer k through exploitative competition with another consumer l, Eq. (6), can be written as $\mathsf{C} < \mathsf{D}\,\mathsf{A}/\mathsf{B}$, or

$$\log_{10}\mathsf{C} - \log_{10}\mathsf{D} - \log_{10}\mathsf{A} + \log_{10}\mathsf{B} < 0, \tag{13}$$

with the four named terms

$$\mathsf{A} = \sum_j H_{jl} - 1,\ \mathsf{B} = \sum_j H_{jl}^2,\ \mathsf{C} = \sum_j H_{jk} - 1,\ \mathsf{D} = \sum_j H_{jk}H_{jl}. \tag{14}$$

Terms A and C can be written as $\mathsf{A} = R_l - 1$ and $\mathsf{C} = R_k - 1$, respectively, and represent the intrinsic growth rates of the two consumers in units of ρ. Term B quantifies intraspecific competition of l, Term D its competition with k (see also Appendix S2).

For random pairs k, l of consumers sampled from the steady state of the deconstructed model formulation, the left-hand side of Eq. (13) follows an approximate truncated normal distribution. In Fig. 4a we show this distribution conditional to base attack rate a_k lying within each of the four quartiles of the steady-state distribution of a (Fig. 3e). While the variance does not depend much on a_k, the mean decreases with increasing a_k, making competitive exclusion by Eq. (13) more likely, consistent with the decreasing trend for mean life time in Fig. 3h. This trend must be due to the dependencies of Terms C and D on a_k, because A and B depend only on competitor l.

Figures 4b,c show the corresponding distributions of the additive contributions $\log_{10}\mathsf{C}$ and $-\log_{10}\mathsf{D}$. The mean of $\log_{10}\mathsf{C}$ *decreases* slightly with increasing a_k (linear regression $\pm$ s.e.: $\log_{10}\mathsf{C} = (-0.200 \pm$

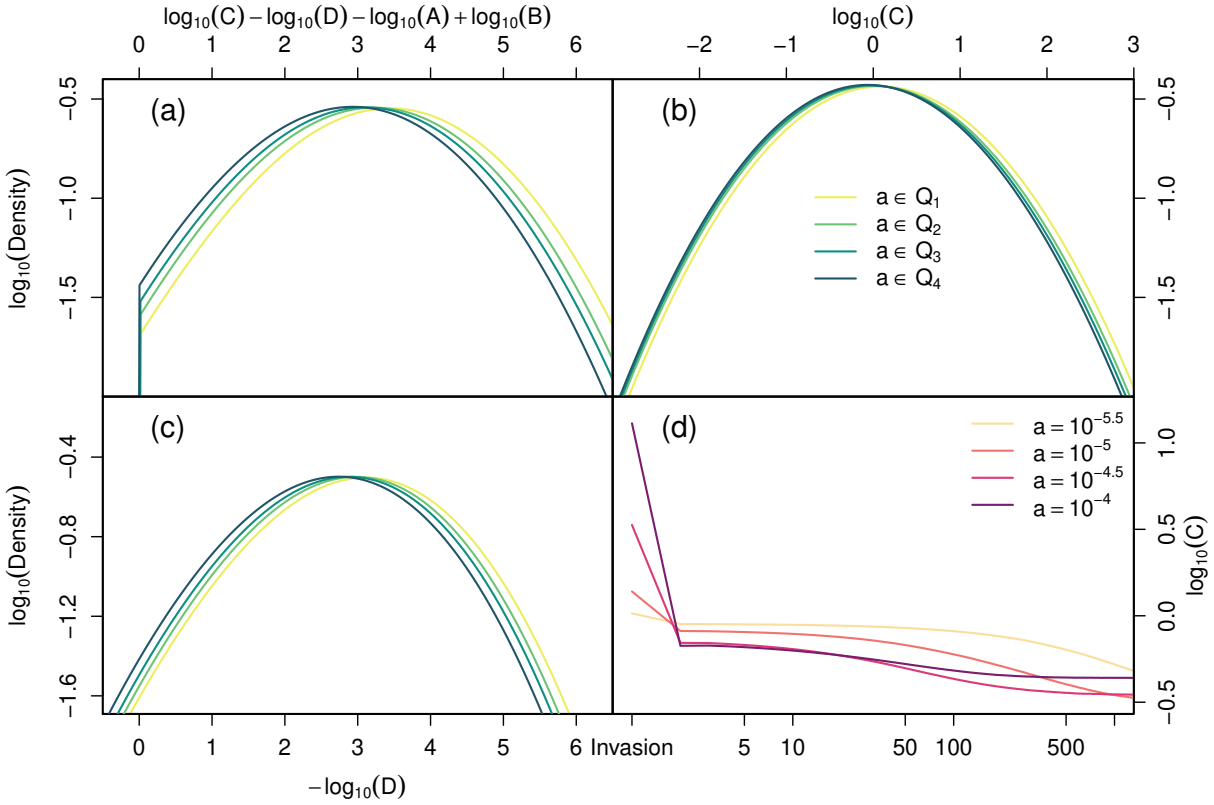

Figure 4: **Components of the condition for consumer competitive in the deconstructed model formulation.** Panels (a) represents the distribution of the left-hand side of condition (13) for competitive exclusion in the steady state of the deconstructed model formulation, panels (b) and (c) two additive contributions defined in Eq. (14). Probability densities were computed using the density function of R with bandwidth parameter set to 0.5. They were computed separately conditional to base attack rate a lying in one of the four quartiles of its steady-state distribution (Q_1-Q_4, see legend). Panel (d) shows how the geometric mean (10^6 replicates) of Terms C changes with each iteration of the serial resource extirpation algorithm of Sec. 3.3, for different base attack rates of the consumer (see Appendix S5 for more detailed results). These results reveal that serial extirpation generates an anomaly in the dependence of Term C (but not D) on a, which makes extirpation of consumers more likely with larger base attack rate a.

$0.002) \times \log_{10} a_k + \text{intercept}$). This is surprising. With attack rates sampled at random following Eq. (4), a linear *increase* of R_k with a_k is expected, implying a slope > 1 for the regression. By contrast, the decline of $-\log_{10} D$ with increasing a_k ($\log_{10} \mathsf{D} = (0.632 \pm 0.006) \times \log_{10} a + \text{intercept}$) is mostly in line with expectations—for H_{jk} sampled at random according to Eq. (4), $\mathsf{D} = \sum_j H_{jk} H_{jl}$ increases linearly with a_k. The key to understanding the surprising decline of mean consumer population lifetime $L(a)$ with increasing a therefore lies in understanding the unexpected absence of an increase of R_k, and so of Term C, with a_k, and why this is not reflected in Term D.

Both R_k and Term D are sums of the attack rates of k over all resources. In Term D the sum contains what are effectively log-normally distributed random weighting factors H_{jl}. These can give prominence to resources j in the sum that contribute little to the unweighted sum R_k, and conversely reduce the weight of the resources that dominating in R_k. This suggests a central role of the main resources of k, hinting at consumer-mediated competitive exclusion by Eq. (8). We follow this lead.

Box 2 A simplified model of serial resource extirpation

The model simulates a single consumer $k = 1$ with base attack rate a_k in a community of $S_\mathrm{R} = 300$ resources. It is described by the following algorithm:

1. Sample sets of S_R scaled attack rates H_{jk} according to Eq. (4) until one is found found that satisfies the invadability criterion, Eq. (5). Continue with this set.
2. Record the initial value of $\mathsf{C} = \sum_j H_{jk} - 1$ (marked "Invasion" in Fig. 4d).
3. Impact: as long as the condition for consumer-mediated competitive exclusion, Eq. (8), is satisfied, remove the resource of j with the largest H_{jk}.
4. Record the value of $\mathsf{C} = \sum_j H_{jk} - 1$.
5. Replace the resources removed in Step 3 with new ones, sampling new values H_{jk} following Eq. (4). If no resource was removed in Step 3, chose a random resource i and re-sample H_{ik}, conditional to satisfaction of the invadability criterion, Eq. (5).
6. Repeat from Step 3 for a predetermined number of iterations.

3.3 Restructuring of resource communities by consumers

To understand how consumer-mediated competitive exclusion affects R_k and C, we devised a further simplification of the deconstructed model. In this model, only one consumer k is considered. It's base attack rate a_k is a model parameter, and the number of resource species is fixed. The model, detailed in Box 2, mimics gradual changes through time in a consumer's resource set in the deconstructed model formulation, but suppresses the possibility of consumer extirpation.

In Fig. 4d we show averages of sequences of $\mathsf{C} = R_k - 1$ through time predicted by this algorithm for four different values of a_k. While at the time of invasion (Step 2 in Box 2) C increases with a_k in line with expectation, this order is reversed by the first iteration of consumer-mediated competitive exclusion (Step 3), which corresponds to the Impact phase of the deconstructed formulation. In subsequent iterations this reversal is maintained and eventually C becomes largely independent of a_k (Fig. S2).

The output of this model until the first execution of Step 3 (Impact) is accessible to mathematical analysis (Appendix S5). We considered the mathematical limit of large resource richness S_R, while keeping the expected Gini-Simpson dietary diversity of consumers at the time of invasion fixed at a value $0 < \nu < 1$ by adjusting the spread σ of the log-normal attack-rate distribution as $\sigma = \nu^{-1}\sqrt{2\ln S_\mathrm{R}}$ (Rossberg *et al.*, 2011; Rossberg, 2013, Ch. 11, 12). For large base attack rates a_k, this leads to

$$\mathsf{C} = R_k - 1 = \sum_j^{S_\mathrm{R}} H_{jk} - 1 = 1 - \nu \tag{15}$$

after Impact on average. Convergence of $R_k - 1$ to this value with increasing S_R is very slow (of order $\mathcal{O}(1/\log S_\mathrm{R})$ or slower), and so the quantitative prediction by Eq. (15) not borne out in practice. But the broader implication of Eq. (15) holds even for moderate S_R: after Impact, C will be of the order of magnitude of one even when the consumer's base attack rate is large (Fig. 4d).

With the value of Term C thus constrained while that of Term D increases with base attack rate on average, the likelihood of competitive exclusion by other consumers increases with a consumer's base attack rate according to Eq. (13). This explains why more aggressive consumers have a shorter mean time to extirpation L (Fig. 3h).

3.4 Summary of mechanism

We can now put together the picture of how prudence evolves in our model. Crucial is that during the Impact phase imprudent consumers (those with high base attack rates) extirpate their main resources through consumers-mediated competitive exclusion. As a result, the basic reproduction number of extant consumers in the model depends only weakly on base attack rate, even though in the initial establishment phase it is proportional to base attack rate. The effect of resource extirpation on the strength of competition with other consumers is weaker, and so less prudent consumers are more likely to get competitively excluded by other consumers. Imprudence thus causes early extirpation on average.

Characteristic of this process is the separation of the ultimate and proximate causes of extirpation of an imprudent consumer (Fig. 1). The *ultimate cause* is extirpation of its resources. This, on its own, however, does not extirpate the consumer. Some other event, the *proximate cause*, needs to push the consumer over the brink. In our model, this can be invasions of immediate competitors or indirect effects resulting from turnover of resource and/or consumer community, driven, e.g., by Pyrrhic competition (inspection of simulations shows that both cases occur). In reality, shifts in environmental conditions, arrival of predators or spread of diseases can equally play this role.

Early extirpation of imprudent consumers interacts with other evolutionary forces (Fig. 3) as follows: ease of establishment in communities increases with increasing base attack rates, but with diminishing returns. Since high base attack rates are not beneficial for the subsequent long-term population survival, a moderate mutation bias can thus prevent attack rate evolution beyond values where invasions become likely. As a result, prudence evolves. As we demonstrate in Appendix S6, "cheaters", who out-compete prudent conspecifics as they invade local communities, do not fundamentally undermined this outcome.

The mechanism described above is essentially different from resource overexploitation through simple monophagous consumer-resource interactions. The latter occurs either during the initial Spread phase of invasions or—in models with non-linear functional responses (Rosenzweig, 1971)—in the course of predator-prey cycles, and is controlled by some lower cutoff for viable resource population biomass ($M_{\min}$ in Eq. (7)). With our choice of $M_{\min}$ such dynamic resource extirpations followed by extirpation of the consumer are rare (Fig. S4). By contrast, new mechanism does not depend on such a cutoff, because it operates in population-dynamical equilibrium.

It is likely that the evolution of prudence previously observed in the size-structured food web models, which include real-world complications such as direct competition amongst producers, omnivory, food-web loops, and phylogenetic patterning (Rossberg *et al.*, 2008; Rossberg, 2013, Sec. 22.3), is driven by the same mechanism. The key element of the new mechanisms, consumer-mediated competitive exclusion, operates in food webs despite all these complications as long as the approximation of linear functional responses applies (Rossberg, 2013, Sec. 15.3).

3.5 The role of the functional response

How then does variation in functional responses affect the mechanism we described? Consumer-mediated competitive exclusion is robust with respect to the introduction of Type II functional responses (Grover & Holt, 1998; Křivan & Eisner, 2006). The phenomenon also persists with moderate adaptive foraging (van Leeuwen *et al.*, 2007), although it disappears in the extreme case of optimal foraging (Křivan & Eisner, 2006).

Predator-dependent functional responses, however, which describe a reduction of per-capita feeding rate with increasing consumer (predator) abundance (Tyutyunov & Titova, 2020), facilitate resource coexistence in situations where consumer-mediated competitive exclusion would otherwise occur (Coblentz & DeLong, 2020). Predator-dependence, which is is empirically well documented (Skalski & Gilliam, 2001; DeLong & Vasseur, 2011; Arditi & Ginzburg, 2012; Stouffer & Novak, 2021), thus offers and alternative route to prudence. However, firstly, this just shifts the problem of explaining consumer-resource coexistence to understanding why and to what extent consumers have evolved to restrain foraging in the presence of competitors. Secondly, with consumers behaviourally restraining themselves, there is again little fitness benefit in excessively high base attack rates, potentially constraining realised base attack rates as a result. Prudence in nature could be realised by mixtures of varying composition between adaptation of based attack rates and predator-dependence of functional responses.

3.6 The analogy with evolution of virulence

Evolution of prudent predation has an analogy in the evolution of the virulence of infectious diseases (Lion & Boots, 2010). Laying out this analogy can contribute to demystifying evolution of prudence. According to the classical theory by Anderson & May (1982), evolutionary stable virulence is the outcome of a trade-off between virulence and transmission rate (Cressler *et al.*, 2016). Virulence, i.e. the mortality of infected hosts, corresponds to inverse population "life time" $1/L(a)$ in our model and transmission rate to population "birth rate" $b(a)$. As for infectious diseases, a trade-off between $L(a)$ and $b(a)$ arises in our model (Fig. 3) that leads to evolutionary stable values for a, $b(a)$, and $L(a)$.

The major difference to current models of evolutionary epidemiology (Cressler *et al.*, 2016) is the inclusion of mutation bias in Eq. (3). For viruses, such bias is well documented (Sanjuán *et al.*, 2004; Silander *et al.*, 2007); its omission in epidemiological models most likely just a nod to parsimony. Indeed, the bias would only shift evolutionary stable virulence to smaller values in most models, without fundamentally affecting mechanisms. In our model this is different. Since $b(a)$ plateaus with increasing a and $L(a)$ declines, $R(a) = b(a)L(a)$ appears to attain a maximum along the a axis, representing an evolutionary stable point even without mutation bias. The corresponding base attack rate a, however, is rather high. It would lead to a decline in resource richness (Rossberg, 2013, Sec. 20.2) and, ultimately, to extirpation of all consumers. Mutation bias is hence a facet of reality our model cannot afford to gloss

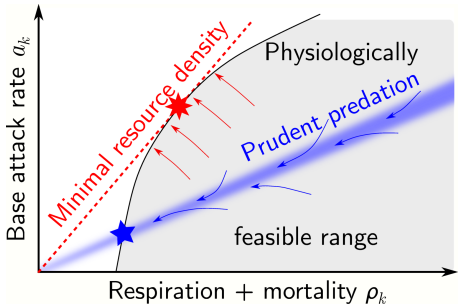

Figure 5: **Prudence and optimisation in evolution.** The figure schematically illustrates evolutionary forces acting on a single, isolated consumer k (red) feeding a single resource, and a polyphagous consumer k embedded in a metacommunity (blue). The area shaded in grey indicates the range of physiologically feasible combinations of attack and respiration rates under *ad libitum* feeding. The isolated monophagous consumer will evolve to minimise the abundance of its resource at equilibrium (arrows), controlled by ρ_k/a_k, leading to an evolutionary optimum as indicated by the eight-pointed star. The polyphagous consumer in a metacommunity will evolve towards prudent predation (range of corresponding ρ_k/a_k values indicated by blue shading) and also to minimise its respiration+mortality rate (arrows) in order to maximise its abundance. The evolutionary endpoint is then given by the five-pointed star. Both endpoints are consistent with observations in so far as they represent the limit of physiologically feasible a_k-ρ_k combinations.

over.

3.7 Prudence and optimisation

Purely ecological mechanisms constrain the basic reproduction number R_k of extant consumers k in our model (Sec. 3.3). Evolved prudence means that, through adaptation of k's phenotype, R_k for newly establishing species is also constrained to values not much larger than 1.

At first sight, such adaptation appears to contradict decades of research demonstrating that organisms have evolved to optimise their metabolism, minimise mortality, and maximise their intrinsic population growth rates. But this apparent contradiction can be resolved.

The metapopulation fitness of species is determined not only by their abilities to invade patches and population survival within patches, but also by the rate of dispersal from one patch to others. This rate is controlled not only by dispersal strategy but also by population size within patches. All else equal, larger populations disperse more propagules.

Population biomass in our model is $\hat{B}_k^{\mathrm{C}} = \alpha_{0k} s B_k^{\mathrm{C}} = \epsilon K s \rho_k^{-1} B_k^{\mathrm{C}}$. In this expression, dimensionless population biomass B_k^{C} is independent of ρ_k for given scaled interaction strengths H_{jl} ($1 \leq j \leq S_{\mathrm{R}}$, $1 \leq l \leq S_{\mathrm{l}}$), and K and s are characteristics of the resources. To increase population size, and hence dispersal, consumers can therefore adapt to minimise ρ_k while at the same time keeping and $R_k = \sum_j^{S_{\mathrm{R}}} H_{jk}$ in the range consistent with prudent predation. (A corresponding argument could be made for assimilation efficiency ϵ.)

Figure 5 schematically compares evolutionary forces and the resulting position of the evolutionary stable strategy in the space spanned by ρ_k and a_k for a prudent consumer (blue) and for a monophagous consumer in an isolated community (red). Crucially, both optima are consistent with empirical observations

that foraging apparatus and strategies are optimised to maximise base attack rates a_k within the limits of given metabolic+mortality costs ρ_k, and that metabolic and mortality costs are minimised under the constraint of maintaining the biological machinery required to retain a given base attack rate a_k.

The difference between the two optima lies in the (true or apparent) quantitative trade-off between ρ_k and a_k, i.e. the slope of the edge of the physiologically feasible range at the optimum in Fig. 5. Empirical work rarely if ever quantifies this trade-off for comparison with theoretical expectations. Prudent predation therefore cannot be dismissed simply on the grounds that metabolism, longevity and foraging are found to be minimised or maximised in nature with some trade-off.

4 What empirical support for our theory looks like

We discussed a range of conceivable mechanisms for consumer-resource coexistence. These include resource survival at metapopulation level, resources winning evolutionary arms races, prudence through predator-dependent functional responses, and evolution of prudence *via* either selection by monophagous boom-bust cycles or the polyphagous mechanism describe here. To test specifically for the polyphagous mechanism, we propose to study three kinds of empirical data:

1. Basic reproduction numbers of resident consumers, to test for ecological constraints on this number.
2. Events surrounding invasive alien consumers, to test for separation of ultimate and proximate causes of selection for prudence.
3. Comparisons of minimum required and actual resource densities, to test for manifest prudence.

Below we provide examples of each. Tests 1 and 2 are specific to the polyphagous mechanism. Test 3 excludes metapopulation-level resource survival and to some extent predator-dependent functional responses.

4.1 Evidence of ecological constraints on basic reproduction number

Our theory predicts an ecological constraint on the basic reproduction number R_k of resident polyphagous consumers k (after their impact phase). This can be tested by studying what fisheries scientists call *stock-recruitment relations* (Fig. 6, thick lines): the functional dependence of the number of newly maturing recruits Rec(SSB) produced by a stock each year on its spawning stock biomass, SSB—the total biomass of sexually mature individuals.

With SSB_0 denoting SSB for the unfished, virgin stock, one defines the *steepness* h (Fig. 6) of Rec(SSB) as

$$h = \frac{\mathrm{Rec}(0.2 \times \mathrm{SSB}_0)}{\mathrm{Rec}(\mathrm{SSB}_0)}. \tag{16}$$

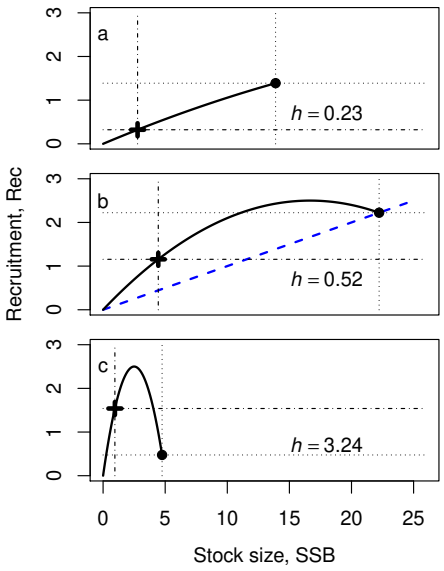

Figure 6: **Stock-recruitment relations and steepness.** The figure illustrates the range of possible stock-recruitment relations (thick lines) that can emerge from a Lotka-Volterra model of a fish stock feeding on a single resource (Appendix S7). Panels a, b, and c, correspond to basic reproduction numbers 1.2, 3, and 20, respectively. Specifically, we evaluated the model of Appendix S7 with $a = 1.2K^{-1}$, $3K^{-1}$, $20K^{-1}$, the other parameters fixed at $s = 1$, $K = 100$, $\epsilon = 0.1$, $\rho = 0.1$, and fishing mortality F varying from 0 up to the value where the fish stock goes extinct. Stock size SSB $=$ SSB_0 and recruitment Rec for the unfished ($F = 0$) community are indicated by a circle and dotted lines, SSB and Rec at 20% of the unfished stock size by a cross and dash-dotted lines. The resulting steepness h, defined as the ratio of the two Rec values, is indicated in each panel. To see why steepness and basic reproduction number are closely related, note that for a virgin stock, and hence along the blue dashed line in Panel b, each adult fish has exactly one recruit offspring on average. Basic reproduction number is the factor by which recruitment lies above this line at minimal abundance, steepness is 0.2 times this factor at $0.2\,\mathrm{SSB}_0$. Observed stock-recruitment relations typically resemble rather Panel b than Panels a or c.

Steepness is closely related to basic reproduction number (Fig. 6). In Appendix S7, we show that for a single stock k feeding on multiple resources in a Lotka-Volterra model

$$h_k = \frac{1}{25}\left(1 + 4R_k\right). \tag{17}$$

The ecological constraint on R_k thus implies a constraint on steepness h_k (see also Myers *et al.*, 1999).

Is this constraint observed? For fish stocks, yes. Following the realisation that steepness attains preferred values across stocks (Punt *et al.*, 1994; McAllister *et al.*, 1994), priors for steepness are now regularly used to estimate stock-recruitment relations for data-poor stocks (Punt & Dorn, 2014). In simple cases, a fixed value for h is used. The assumption that steepness has some preferred value is also implicitly in rules of thumb that estimate the fishing mortality rate generating maximum sustainable yield as a constant multiple of the natural mortality rate of adults (Beddington & Kirkwood, 2005), which are surprisingly accurate (Zhou *et al.*, 2012).

This preference for steepness to attain certain values could never be explained (Myers *et al.*, 1999; He *et al.*, 2006). Ginzburg *et al.* (2010) argued that, for annual or age-structured populations (Tuljapurkar *et al.*, 1994), periodic or chaotic oscillations can set in at large R_k, independent of the detailed nature of density dependence, thus potentially selecting against large R_k. However, for these such oscillations to lead to extirpations, and so selection, their amplitude would need to be much larger than anything observed in the fisheries context. Our theory provides a more natural explanation.

Unfortunately, quantitative comparisons of steepness are possible only for a fixed functional form of the fitted stock-recruitment relation (Munyandorero, 2020), and we are unaware of systematic studies using Lotka-Volterra (or "Schaefer") models. Typically, the Beverton-Holt model is used (Rec $= c_1\mathrm{SSB}/(1 + c_2\mathrm{SSB})$ with parameters c_1, c_2), for which steepness priors tend to have a mode near $h = 0.8$ (McAllister *et al.*, 1994; Zhou *et al.*, 2012; Shertzer & Conn, 2012; Thorson *et al.*, 2019; Munyandorero, 2020). Remarkably, this mode near $h = 0.8$ was also found in a size-structured marine food-web model where interacting fish and their resources were explicitly modelled, permitting the mechanism described in Sec. 3.3 to unfold (Rossberg *et al.*, 2013).

4.2 Evidence of operation of the polyphagous selection mechanism

By definition, invasive alien species cause harm to the ecosystems they invade. Often, this is through predation or grazing. Such harmful invasive consumers appear to have base attack rates too high for the invaded ecosystems to sustain. Our theory predicts a series of telltale signatures that should be observable when such imprudent alien polyphagous consumers invade local communities:

1. Fast initial population growth, indicative of an imprudent alien consumer.

2. A strong impact on the resource community, involving resource extirpations or resource depletion

Table 2: Examples of observed signatures of the operation of the proposed mechanism selecting for prudence as being reported for invasive alien consumers. For detailed explanation of signatures, see text.

Invasion Event	Signature				Key References
	1. Fast Growth	2. Resource Extirpation	3. Adjustment	4. Disappearance	
Comb jellyfish (*Mnemiopsis leidyi*) in the Black Sea	yes	yes	yes	decline	Kideys 2002
Indo-Pacific lionfish (*Pterois volitans/miles*) in Gulf of Mexico	yes	yes	yes	decline	Côté & Smith 2018 Harris *et al.* 2020
Signal crayfish (*Pacifastacus leniusculus*) in Swedish lakes	yes	yes	yes	yes	Sandström *et al.* 2014 Ruokonen *et al.* 2014
Argentine ant (*Linepithema humile*) in New Zealand	yes	yes	?	yes	Cooling *et al.* 2012 Tillberg *et al.* 2007

to low levels sustained by immigration (i.e. mass effects, Shmida & Wilson 1985). This might go along with exclusion of competing consumers.

3. A halt in population growth, potentially with subsequent decline, after which the invader's population stabilises.

4. Further local decline or even extirpation of the invader's population, explained through the (re-)emergence of competitors, other rather unsuspicious causes, or unexplained.

That is, we are not only predicting "population crashes of established introduced species", reviewed by Simberloff & Gibbons (2004), but a more detailed pattern that evidences the temporal separation of the ultimate cause (2.) from the proximate cause (4.) of population collapse. This separation is highly specific to the mechanism we propose. In particular, it does not arise with the monophagous counterpart.

We shall discuss four well-studied examples of invasive alien consumers where these signatures have been fully or partially documented (Tab. 2). This serves not only to illustrate how these signatures manifest themselves in the field but also demonstrates that observation of what we predict is not unheard of. A careful meta-analysis would be required to establish how common documentation of these signatures is and to what extent absence of their documentation is due to incomplete observation or reporting.

4.2.1 Comb jellyfish in the Black Sea

The comb jelly *Mnemiopsis leidyi* is a "voracious zooplanktonic predator" (Kideys, 2002), known to depress both abundance and diversity of mezoplankton (Shiganova, 1998; Fiori *et al.*, 2019). After arriving in the Black Sea through ballast water, its outbreak in 1989 (with density $> 1\,\mathrm{kg\,m^{-2}}$) led to a sharp decline of anchovies, previously the dominating planktivores in the Black Sea, a result of both resource competition and predation of larvae (Kideys, 2002). Over the subsequent three years, however,

Mnemiopsis declined about five-fold and anchovy catches recovered to their previous levels. Whatever resources fuelled the 1989 outbreak had been exhausted. Between 1992 and 1998 *Mnemiopsis* coexisted with anchovy at this lower abundance (Kideys *et al.*, 2000). Predation by the invading ctenophore *Beroe* (*B. ovata* or *B. cucumis*), which appeared in 1997, led to a further sharp decline of *Mnemiopsis* in 1999. Because *Beroe* feeds almost exclusively on *Mnemiopsis* (Finenko *et al.*, 2001), it cannot entirely extirpate its prey. Currently, the two jellyfish therefore appear to persist in the Black Sea at low abundance.

4.2.2 Lionfish in the Gulf of Mexico

Indo-Pacific lionfish *Pterois volitans/miles* grow and reproduces fast (Côté & Smith, 2018), deter predators with venomous spines (Vetrano *et al.*, 2002; Côté & Smith, 2018), have high physiological tolerance, and are effective predators, as they appear inconspicuous to their prey (Lönnstedt & McCormick, 2013). The course of their invasion of the Northern Gulf of Mexico and neighbouring areas since 1985 is exceptionally well studied (Côté & Smith, 2018; Harris *et al.*, 2020). Prey extirpation by lionfish has been documented in controlled field experiments (Ingeman, 2016).

In 2018, Côté & Smith found first indications that the worst-case scenario of lionfish invasion envisioned by Albins & Hixon (2013), "in which most reef-fish biomass is converted to lionfish biomass, leaving invaded reefs depauperate of native fishes", would not materialise. Benkwitt *et al.* (2017) reported for 64 unmanaged and unfished reefs in the Bahamas how lionfish populations first rapidly increased (70.6% per year), plateaued for between 2 and > 7 years, and then, in some case, their unexplained declines (by up to 99% over a 4-year period). Populations of the Nassau grouper (*Epinephelus striatus*), a comparable native predator, varied much less. Similarly, Harris *et al.* (2020) detailed what they called a "precipitous declines" of lionfish density in the Northern Gulf of Mexico over the period 2017-2019 (by up to 77-79%). Harris *et al.* associated this decline with an ulcerative skin disease observed on lionfish, but since this peaked in 2017 while the decline continued into 2019, other factors might also play a role.

4.2.3 Signal crayfish in Swedish lakes

Sandström *et al.* (2014) documented 40 years of population dynamics of North American signal crayfish (*Pacifastacus leniusculus*) that were introduced into 44 Swedish lakes. Most populations exhibited the rapid increase characteristic of invasive species, after which populations sizes stabilised. Yet, 41% of these populations collapsed after an average of 10.8 years without recovering. The authors considered and dismissed presence of predatory eel (*Anguilla anguilla*) and of crayfish plague (*Aphanomyces astaci*) to explain the collapses. Instead, they found subtle statistical effects of temperature and year of stocking. Based on evidence of strong density dependence in population time series and because it is known from Finnish lakes that *P. leniusculus* modifies and depauperates its macroinvertebrate prey community (Ruokonen *et al.*, 2014), Sandström *et al.* (2014) offer resource overexploitation as a likely mechanistic

explanation of the collapses.

4.2.4 Argentine ants in New Zealand

An example from the terrestrial realm is provided by populations of the Argentine ant (*Linepithema humile*) in New Zealand (Cooling *et al.*, 2012). In the words of Cooling *et al.*, "Introduced populations form high-density, widespread, highly aggressive, unicolonial populations and can deleteriously influence native communities (Holway *et al.*, 2002)." While collapse and extirpation of invasive ant populations are a common phenomenon (Lester & Gruber, 2016), attribution of mechanisms can be hampered by insufficient understanding of ant diet and feeding behaviour. As Holway *et al.* (2002) point out, predation and scavenging must be distinguished. Noteworthy are therefore observations by Tillberg *et al.* (2007) that the trophic position of invading *L. humile* is highest at the invasion front and declines with the duration of site occupation, falling well below the trophic position of *L. humile* in its native range. This evidences resource depletion through predation that scavenging cannot explain. When Abril *et al.* (2007) found in invaded natural areas that most of the solid food of *L. humile* was dead and dehydrated, this might plausibly have been because *L. humile* had already extirpated their preferred life prey.

Studying 150 sites with recorded *L. humile* presence in New Zealand, Cooling *et al.* (2012) found that 40% of populations had collapsed, with survival time in the rage of 10-18 years. Of the remaining populations, "many had shrunk from numerous nests covering multiple hectares with extremely high abundances to just one or two nests covering a very small area with low worker densities." At infested sites, richness and abundance of other ant species was depressed but recovered after *L. humile* collapsed, providing additional indirect evidence of severe resource depletion by *L. humile*.

4.3 Evidence of manifest prudence

From laboratory measurements of attack rate a_{jk} for preferred resources j of a consumer k, its assimilation efficiency ϵ, and respiration+mortality rate ρ_k one can determine the minimum resource biomass $\rho_k/(\epsilon a_{jk})$ or, in practice, biomass density that k requires to sustain its population. When this is similar to the resource density in k's native habitat, we call this *manifest prudence*; it is the outcome predicted by our theory. If native resource density is much higher than this a mechanism different from what we propose must be enabling consumer-resource coexistence. In cases where comparisons of absolute values of minimum required and native resource density are not possible, one can test for proportionality of the two quantities across contrasting groups of organisms.

In pelagic ecology $a_{jk} = m_k^{-1} s_{jk}$ is called the *maximum specific clearance rate*, and determined from consumer biomass m_k and the maximum slope s_{jk} (dimension Volume/Time) or similar of a measured functional response. Marine ecologists have often studied whether pelagic consumers are food limited, and the question to what extend food is sufficient for survival got addressed along the way. In this

context Huntley & Boyd (1984) introduced $C_{\mathrm{m}} = \rho_k/(\epsilon a_{jk})$ as the "maintenance food concentration". The contribution of mortality to ρ_k is not usually considered, thus underestimating the true minimum requirement. Despite this, true native resource densities tend to be lower than C_{m} (Mullin & Brooks, 1976; Huntley & Boyd, 1984; Huntley, 1992; Hirst & Bunker, 2003)!

To reconcile this discrepancy, it has been argued that pelagic consumers might be able to exploit higher then average resource density, since resource distribution is patchy on the relevant scales (Mullin & Brooks, 1976; Huntley, 1992). Whatever the explanation, an abundance of data suggest that clearance or attack rates of marine pelagic consumers are not much higher than required to sustain their population. Marine pelagic consumers are manifestly prudent.

4.3.1 Trends across ocean biogeographic regions

Huntley & Boyd (1984), for example, executed the program above for marine herbivorous zooplankton, paying attention to include only studies conducted "at temperatures encountered in the natural habitat" of study organisms. Temperatures varied between 0 and 30°C, covering most global ocean-climatic zones. Higher sea-surface temperatures reduce mixing of the water column, and so nutrient supply and phytoplankton density.

Huntley & Boyd compared maintenance food concentration C_{m} with ranges of concentrations of particulate organic carbon (POC) observed in studies spanning 0-25°C water temperature, while distinguishing between "coastal" and "oceanic" waters. For organisms of 0.1 mg dry mass (the size of the copepod *Calanus pacificus*) C_{m} varied by a factor 23 from $0.022\,\mathrm{mg\,L^{-1}}$ at 25°C to $0.50\,\mathrm{mg\,L^{-1}}$ at 0°C. This temperature dependence tracked the lower ends of the oceanic POC concentration ranges. Coastal POC concentrations where higher.

The strong temperature dependence of C_{m} was mostly driven by a temperature dependence of a_{jk}. Between 0 and 25°C, a_{jk} increased by a factor 126 for 0.1 mg organisms. As a measure for the strength of temperature dependence, this corresponds to a Q10 value of $126^{10/(25-0)} = 6.9$. Since Q10 for the intraspecific temperature dependence of clearance and other physiological rates of zooplankton lies in the range 1.5-4 (average: 2.8) (Hansen *et al.*, 1997), this large Q10 for a_{jk} is unlikely to be explained on physiological grounds. More plausibly, the large interspecific Q10 for a_{jk} reflects adaptation of zooplankton species to different characteristic resource densities—ultimately controlled by ocean physics.

Interestingly, Huntley & Boyd's Q10 = 2.0 for respiration is in the expected range. This is consistent with the expectation from Sec. 3.7 that ρ_k will be at the physiological limit while a_{jk} is adjusted for prudence.

Remarkable in this context is also a meta-analysis by Kiørboe (2011b) showing that the geometric mean specific clearance rate of freshwater cladocerans (water fleas) is lower by an approximate factor 10 than that of marine copepods (which occupy a similar ecological niche). This is the trend expected from

prudence, because in freshwater nutrients and food tend to be more abundant.

4.3.2 Trends across life forms

Kiørboe & Hirst (2014) conducted a meta-analysis of respiration ρ_k and specific clearance rates a_{jk} of marine pelagic species spanning a factor 10^{15} in body mass. *Within* major taxonomic and life-form groups (flagellates, ciliates, calanoid copeopods, non-calanoid copeopods, euphasids, cnidaria & ctenophores, tunicates, pisces) they found that the scaling of both rates is consistent with $-1/4$ power laws. The lead coefficients ("intercepts") of the power laws, however, differed between taxonomic groups in such a way that both scaling exponents, when evaluated *across* all groups and body sizes, were close to 0.

It is unsurprising that two organisms of the same size but from different taxonomic groups feed and metabolise at somewhat different rates (Kiørboe, 2011a). What surprised Kiørboe & Hirst (2014) was that the changes between groups in the lead coefficients size for ρ_k and for a_{jk} were of similar, such that $\rho_k/(\epsilon a_{jk})$ remained similar across groups.

Can prudent predation explain this? In marine pelagic ecosystems biomass is approximately evenly distributed over the logarithmic body size axis (Sheldon *et al.*, 1972), implying an approximately equal density of food available to organisms of all sizes. To be precise, biomass slightly declines with body mass (Rossberg *et al.*, 2019), but so does species richness. The two effects plausibly compensate each other such that the biomass density of a consumer's preferred resources is independent of consumer body mass. Manifest prudence then means invariance of $\rho_k/(\epsilon a_{jk})$ across body size, as documented by Kiørboe & Hirst (2014).

Remarkably, the variation of ρ_k around the overall geometric mean ($\approx 0.05\,(\mathrm{gC/gC})\,\mathrm{day}^{-1}$) found by Kiørboe & Hirst (2014) is smaller than that of a_{jk}, and this mean value of ρ_k is observed similarly across all domains of life (Makarieva *et al.*, 2008). This, too, agrees with our expectation (Sec. 3.7) that ρ_k will be at the physiological limit while a_{jk} is adjusted for prudence.

5 Prudent predation - the way forward

Both, the theoretical and the empirical pictures we have drawn of the polyphagous mechanism for evolution of prudence remain incomplete. Our theory represents several elements implicitly, including the metacommunity (O'Sullivan *et al.*, 2020), continuity of space (Goodnight *et al.*, 2008), trophic trait matching (Appendix S1), and evolution on the generational timescale (Mitteldorf *et al.*, 2002). Simulations making these elements explicit would be challenging but feasible, and useful for confirming their interaction in the ways we predict. And while we presented empirical evidence of predicted processes (Sec. 4.2) and outcomes (Sec. 4.1, 4.3), different evidence related to different systems. Future research should address these gaps.

What gives us confidence in the theory despite these caveats are its reliance on generic ecological principles and its tremendous explanatory power. All three specific patterns it predicts (preferred steepness values, delayed decline of invasive alien consumers and manifest prudence) have long been noticed but remained hitherto unexplained. Evolved prudence offers explanations for all three apparently unrelated loose ends or, in the words of Kuhn (1962), "anomalies". A dismissal of evolved prudent predation would not only reopen the old question of how consumers and resources coexist in nature, it would also forfeit its potential for theoretical unification.

To both sceptics and enthusiasts of our theory we suggest more wide-ranging testing for the predicted patterns across biota. For example, the analysis by Kiørboe & Hirst (2014) discussed in Sec. 4.3.2 could be expanded to include biogeography (Sec. 4.3.1), and databases such as FoRAGE (Uiterwaal *et al.*, 2018) might permit its extension beyond marine pelagic systems.

Acknowledgements We thank Andrew G. Hirst, Vincent A. A. Jansen, Andrew R. Leitch, André M. de Roos and J.C.D. (Chris) Terry for discussion and comments on previous versions of this contribution. Not all necessarily agreed. Research supported by UK's Natural Environment Research Council (NE/T003510/1).

References

Abril, S., Oliveras, J. & Gómez, C. (2007). Foraging activity and dietary spectrum of the Argentine ant (Hymenoptera: Formicidae) in invaded natural areas of the northeast Iberian Peninsula. *Environ. Entomol.*, 36, 1166–1173.

Albins, M.A. & Hixon, M.A. (2013). Worst case scenario: Potential long-term effects of invasive predatory lionfish (*Pterois volitans*) on Atlantic and Caribbean coral-reef communities. *Environ. Biol. Fish*, 96, 1151–1157.

Anderson, R.M. & May, R.M. (1982). Coevolution of hosts and parasites. *Parasitology*, 85, 411–426.

Arditi, R. & Ginzburg, L.R. (2012). *How Species Interact: Altering the Standard View on Trophic Ecology.* Oxford University Press.

Beddington, J.R. & Kirkwood, G.P. (2005). The estimation of potential yield and stock status using life-history parameters. *Phil. Trans. R. Soc. Lond. B*, 360, 163–170.

Benkwitt, C.E., Albins, M.A., Buch, K.L., Ingeman, K.E., Kindinger, T.L., Pusack, T.J., Stallings, C.D. & Hixon, M.A. (2017). Is the lionfish invasion waning? Evidence from The Bahamas. *Coral Reefs*, 36, 1255–1261.

Bersier, L.F. & Kehrli, P. (2008). The signature of phylogenetic constraints on food-web structure. *Ecol. Complex.*, 5, 132–139.

Caldarelli, G., Higgs, P.G. & McKane, A.J. (1998). Modelling coevolution in multispecies communities. *J. Theor. Biol.*, 193, 345–358.

Castellano, D., Macià, M.C., Tataru, P., Bataillon, T. & Munch, K. (2019). Comparison of the full distribution of fitness effects of new amino acid mutations across great apes. *Genetics*, 213, 953–966.

Coblentz, K.E. & DeLong, J.P. (2020). Predator-dependent functional responses alter the coexistence and indirect effects among prey that share a predator. *Oikos*, 129, 1404–1414.

Cooling, M., Hartley, S., Sim, D.A. & Lester, P.J. (2012). The widespread collapse of an invasive species: Argentine ants (*Linepithema humile*) in New Zealand. *Biol. Lett.*, 8, 430–433.

Côté, I.M. & Smith, N.S. (2018). The lionfish *Pterois* sp. invasion: Has the worst-case scenario come to pass? *J. Fish Biol.*, 92, 660–689.

Cressler, C.E., McLeod, D.V., Rozins, C., van den Hoogen, J. & Day, T. (2016). The adaptive evolution of virulence: A review of theoretical predictions and empirical tests. *Parasitology*, 143, 915–930.

Dawkins, R. & Krebs, J.R. (1979). Arms races between and within species. *Proc. R. Soc. Lond. B*, 205, 489–511.

DeLong, J.P. & Vasseur, D.A. (2011). Mutual interference is common and mostly intermediate in magnitude. *BMC Ecology*, 11, 1.

Dempster, J.P. (1971). The population ecology of the Cinnabar Moth, *Tyria jacobaeae* L. (Lepidoptera, Arctiidae). *Oecologia*, 7, 26–67.

Dornelas, M., Gotelli, N.J., McGill, B., Shimadzu, H., Moyes, F., Sievers, C. & Magurran, A.E. (2014). Assemblage time series reveal biodiversity change but not systematic loss. *Science*, 344, 296–299.

Dudley, S.A. (2015). Plant cooperation. *AoB PLANTS*, 7.

Eber, S. & Brandl, R. (1994). Ecological and genetic spatial patterns of *Urophora cardui* (Diptera: Tephritidae) as evidence for population structure and biogeographical processes. *J. Anim. Ecol.*, 63, 187–199.

Eklöf, A. & Stouffer, D.B. (2016). The phylogenetic component of food web structure and intervality. *Theor. Ecol.*, 9, 107–115.

Eyre-Walker, A. & Keightley, P.D. (2007). The distribution of fitness effects of new mutations. *Nat. Rev. Genet.*, 8, 610–618.

Finenko, G.A., Anninsky, B.E., Romanova, Z.A., Abolmasova, G.I. & Kideys, A.E. (2001). Chemical composition, respiration and feeding rates of the new alien ctenophore, *Beroe ovata*, in the Black Sea. *Hydrobiologia*, 451, 177–186.

712 Fiori, E., Benzi, M., Ferrari, C.R. & Mazziotti, C. (2019). Zooplankton community structure before and
713 after *Mnemiopsis leidyi* arrival. *J Plankton Res*, 41, 803–820.

714 Fleischer, S.R., terHorst, C.P. & Li, J. (2018). Pick your trade-offs wisely: Predator-prey eco-evo
715 dynamics are qualitatively different under different trade-offs. *J. Theor. Biol.*, 456, 201–212.

716 Fung, T., Farnsworth, K.D., Reid, D.G. & Rossberg, A.G. (2015). Impact of biodiversity loss on
717 production in complex marine food webs mitigated by prey-release. *Nat. Commun.*, 6, 6657.

718 Gause, G. (1934). Experimental analysis of Vito Volterra's mathematical theory of the struggle for
719 existence. *Sci. N. Y. NY*, 79, 16–17.

720 Gilpin, M.E. (1975). *Group Selection in Predator-Prey Communities*. Princeton University Press.

721 Ginzburg, L.R., Burger, O. & Damuth, J. (2010). The May threshold and life-history allometry. *Biol.*
722 *Lett.*, 6, 850–853.

723 Goodnight, C., Rauch, E., Sayama, H., de Aguiar, M.A.M., Baranger, M. & Bar-Yam, Y. (2008).
724 Evolution in spatial predator-prey models and the "prudent predator": The inadequacy of steady-state
725 organism fitness and the concept of individual and group selection. *Complexity*, 13, 23–44.

726 Grainger, T.N., Levine, J.M. & Gilbert, B. (2019). The invasion criterion: A common currency for
727 ecological research. *Trends Ecol. Evol.*, 34, 925–935.

728 Grover, J.P. & Holt, R.D. (1998). Disentangling resource and apparent competition: Realistic models
729 for plant-herbivore communities. *J. Theor. Biol.*, 191, 353–376.

730 Hansen, P.J., Bjørnsen, P.K. & Hansen, B.W. (1997). Zooplankton grazing and growth: Scaling within
731 the 2-2,000-μm body size range. *Limnol. Oceanogr.*, 42, 687–704.

732 Haraguchi, Y. & Sasaki, A. (2000). The evolution of parasite virulence and transmission rate in a spatially
733 structured population. *J. Theor. Biol.*, 203, 85–96.

734 Harris, H.E., Fogg, A.Q., Allen, M.S., Ahrens, R.N.M. & Patterson, W.F. (2020). Precipitous declines
735 in northern Gulf of Mexico invasive lionfish populations following the emergence of an ulcerative skin
736 disease. *Sci. Rep.*, 10, 1934.

737 Hastings, A. (1977). Spatial heterogeneity and the stability of predator-prey systems. *Theor. Popul.*
738 *Biol.*, 12, 37–48.

739 He, X., Mangel, M. & MacCall, A. (2006). A prior for steepness in stock-recruitment relationships, based
740 on an evolutionary persistence principle. *Fish. Bull.*, 104, 428–433.

741 Hilborn, R. (1975). The effect of spatial heterogeneity on the persistence of predator-prey interactions.
742 *Theor. Popul. Biol.*, 8, 346–355.

743 Hirst, A.G. & Bunker, A.J. (2003). Growth of marine planktonic copepods: Global rates and patterns
744 in relation to chlorophyll *a*, temperature, and body weight. *Limnol. Oceanogr.*, 48, 1988–2010.

745 Hirt, M.R., Tucker, M., Müller, T., Rosenbaum, B. & Brose, U. (2020). Rethinking trophic niches: Speed
746 and body mass colimit prey space of mammalian predators. *Ecol. Evol.*, 10, 7094–7105.

747 Ho, H.C., Tylianakis, J.M., Zheng, J.X. & Pawar, S. (2019). Predation risk influences food-web structure
748 by constraining species diet choice. *Ecol. Lett.*, 22, 1734–1745.

749 Holling, C.S. (1959). The components of predation as revealed by a study of small-mammal predation
750 of the European pine sawfly. *Can. Entomol.*, 91, 293–320.

751 Holt, R.D. (1977). Predation, apparent competition, and the structure of prey communities. *Theor.*
752 *Popul. Biol.*, 12, 197–229.

753 Holway, D.A., Lach, L., Suarez, A.V., Tsutsui, N.D. & Case, T.J. (2002). The causes and consequences
754 of ant invasions. *Annu. Rev. Ecol. Syst.*, 33, 181–233.

755 Huffaker, C. (1958). Experimental studies on predation: Dispersion factors and predator-prey oscillations.
756 *Hilgardia*, 27, 343–383.

757 Huntley, M. & Boyd, C. (1984). Food-limited growth of marine zooplankton. *Am. Nat.*, 124, 455–478.

758 Huntley, M.E. (1992). Temperature-dependent production of marine copepods: A global synthesis. *Am.*
759 *Nat.*, 140, 201–242.

760 Ingeman, K.E. (2016). Lionfish cause increased mortality rates and drive local extirpation of native prey.
761 *Mar. Ecol. Prog. Ser.*, 558, 235–245.

762 Jansen, V.A.A. (2011). On kin and group selection, and the haystack model. In: *The Mathematics*
763 *of Darwin's Legacy* (eds. Chalub, F.A.C.C. & Rodrigues, J.F.). Springer, Basel, Mathematics and
764 Biosciences in Interaction, pp. 139–157.

765 Johst, K. & Schöps, K. (2003). Persistence and conservation of a consumer – resource metapopulation
766 with local overexploitation of resources. *Biol. Conserv.*, 109, 57–65.

767 Kideys, A.E. (2002). Fall and rise of the Black Sea ecosystem. *Science*, 297, 1482–1484.

768 Kideys, A.E., Kovalev, A.V., Shulman, G., Gordina, A. & Bingel, F. (2000). A review of zooplankton
769 investigations of the Black Sea over the last decade. *J. Mar. Syst.*, 24, 355–371.

770 Kiørboe, T. (2011a). How zooplankton feed: Mechanisms, traits and trade-offs. *Biol. Rev.*, 86, 311–339.

771 Kiørboe, T. (2011b). What makes pelagic copepods so successful? *J. Plankton Res.*, 33, 677–685.

772 Kiørboe, T. & Hirst, A.G. (2014). Shifts in mass scaling of respiration, feeding, and growth rates across
773 life-form transitions in marine pelagic organisms. *Am. Nat.*, 183, E118–E130.

774 Kirk, K.L. (1998). Enrichment can stabilize population dynamics: Autotoxins and density dependence.
775 *Ecology*, 79, 2456–2462.

776 Křivan, V. & Eisner, J. (2006). The effect of the Holling type II functional response on apparent
777 competition. *Theor. Popul. Biol.*, 70, 421–430.

778 Kuhn, T.S. (1962). *The Structure of Scientific Revolutions*. vol. 2 of *International Encyclopedia of*
779 *Unified Science*. University of Chicago Press, Chicago, IL.

780 Law, R. & Morton, R.D. (1996). Permanence and the assembly of ecological communities. *Ecology*, 77,
781 762–775.

782 van Leeuwen, E., Jansen, V.a.A. & Bright, P.W. (2007). How population dynamics shape the functional
783 response in a one-predator–two-prey system. *Ecology*, 88, 1571–1581.

784 Lester, P.J. & Gruber, M.A.M. (2016). Booms, busts and population collapses in invasive ants. *Biol.*
785 *Invasions*, 18, 3091–3101.

786 Lindeman, R.L. (1942). The trophic-dynamic aspect of ecology. *Ecology*, 23, 399–417.

787 Lion, S. & Boots, M. (2010). Are parasites "prudent" in space? *Ecol. Lett.*, 13, 1245–1255.

788 Lion, S., Jansen, V.A.A. & Day, T. (2011). Evolution in structured populations: Beyond the kin versus
789 group debate. *Trends Ecol. Evol.*, 26, 193–201.

790 Lion, S. & Metz, J.A.J. (2018). Beyond R_0 maximisation: On pathogen evolution and environmental
791 dimensions. *Trends Ecol. Evol.*, 33, 458–473.

792 Lockwood, J.L., Hoopes, M.F. & Marchetti, M.P. (2013). *Invasion Ecology*. John Wiley & Sons,
793 Incorporated, Hoboken, United Kingdom.

794 Lönnstedt, O.M. & McCormick, M.I. (2013). Ultimate predators: Lionfish have evolved to circumvent
795 prey risk assessment abilities. *PLoS ONE*, 8, e75781.

796 MacArthur, R. (1969). Species packing, and what competition minimizes. *Proc. Natl. Acad. Sci. U. S.*
797 *A.*, 64, 1369–1371.

798 Makarieva, A.M., Gorshkov, V.G., Li, B.L., Chown, S.L., Reich, P.B. & Gavrilov, V.M. (2008). Mean
799 mass-specific metabolic rates are strikingly similar across life's major domains: Evidence for life's
800 metabolic optimum. *Proc. Natl. Acad. Sci. U. S. A.*, 105, 16994.

Maynard Smith, J. & Slatkin, M. (1973). The stability of predator-prey systems. *Ecology*, 54, 384–391.

McAllister, M.K., Pikitch, E.K., Punt, A.E. & Hilborn, R. (1994). A Bayesian approach to stock assessment and harvest decisions using the sampling/importance resampling algorithm. *Can. J. Fish. Aquat. Sci.*, 51, 2673–2687.

Messinger, S.M. & Ostling, A. (2013). Predator attack rate evolution in space: The role of ecology mediated by complex emergent spatial structure and self-shading. *Theor. Popul. Biol.*, 89, 55–63.

Mitteldorf, J., Croll, D.H. & Ravela, S.C. (2002). Multilevel selection and the evolution of predatory restraint. In: *Proceedings of the Eighth International Conference on Artificial Life*. MIT Press, Cambridge, MA, USA, ICAL 2003, pp. 146–152.

Morozov, A. & Petrovskii, S. (2013). Feeding on multiple sources: Towards a universal parameterization of the functional response of a generalist predator allowing for switching. *PLoS ONE*, 8, e74586.

Mullin, M.M. & Brooks, E.R. (1976). Some consequences of distributional heterogeneity of phytoplankton and zooplankton1. *Limnol. Oceanogr.*, 21, 784–796.

Munyandorero, J. (2020). Inferring prior distributions of recruitment compensation metrics from life-history parameters and allometries. *Can. J. Fish. Aquat. Sci.*, 77, 295–313.

Myers, R.A., Bowen, K.G. & Barrowman, N.J. (1999). Maximum reproductive rate of fish at low population sizes. *Can. J. Fish. Aquat. Sci.*, 56, 2404–2419.

Nicholson, A.J. (1933). Supplement: The balance of animal populations. *J. Anim. Ecol.*, 2, 131–178.

Nicholson, A.J. & Bailey, V.A. (1935). The balance of animal populations.—Part I. *Proc. Zool. Soc. Lond.*, 105, 551–598.

Nowak, M.A. (2012). Evolving cooperation. *J. Theor. Biol.*, 299, 1–8.

O'Sullivan, J.D., Terry, J.C.D. & Rossberg, A.G. (2020). Intrinsic ecological dynamics drive biodiversity turnover in model metacommunities. *bioRxiv*, p. 2020.05.22.110262. Accepted by *Nat. Commun.*

Pawar, S., Dell, A.I. & Van M. Savage (2012). Dimensionality of consumer search space drives trophic interaction strengths. *Nature*, 486, 485–489.

Pels, B., de Roos, A.M. & Sabelis, M.W. (2002). Evolutionary dynamics of prey exploitation in a metapopulation of predators. *Am. Nat.*, 159, 172–189.

Persson, A., Hansson, L.A., Brönmark, C., Lundberg, P., Pettersson, L.B., Greenberg, L., Nilsson, P.A., Nyström, P., Romare, P. & Tranvik, L. (2001). Effects of enrichment on simple aquatic food webs. *Am. Nat.*, 157, 654–669.

Pimentel, D., Nagel, W.P. & Madden, J.L. (1963). Space-time structure of the environment and the survival of parasite-host systems. *Am. Nat.*, 97, 141–167.

Pomiankowski, A., Iwasa, Y. & Nee, S. (1991). The evolution of costly mate preferences I. Fisher and biased mutation. *Evolution*, 45, 1422–1430.

Portalier, S.M.J., Fussmann, G.F., Loreau, M. & Cherif, M. (2019). The mechanics of predator–prey interactions: First principles of physics predict predator–prey size ratios. *Funct. Ecol.*, 33, 323–334.

Post, W.M. & Pimm, S.L. (1983). Community assembly and food web stability. *Math. Biosci.*, 64, 169–192.

Punt, A., McAllister, M., Pikitch, E. & Hilborn, R. (1994). Stock assessment and decision analysis for hoki (*Mawwonus novaezelandiae*) for 1994. New Zealand Fisheries Assessment Research Document 94/13, MAF Fisheries, N.Z. Ministry of Agriculture and Fisheries.

Punt, A.E. & Dorn, M. (2014). Comparisons of meta-analytic methods for deriving a probability distribution for the steepness of the stock–recruitment relationship. *Fish. Res.*, 149, 43–54.

Rand, D.A., Keeling, M. & Wilson, H.B. (1995). Invasion, stability and evolution to criticality in spatially extended, artificial host-pathogen ecologies. *Proc. R. Soc. B*, 259, 55–63.

Rauch, E.M., Sayama, H. & Bar-yam, Y. (2003). Dynamics and Genealogy of Strains in Spatially Extended Host–Pathogen Models. *J. Theor. Biol.*, 221, 655–664.

Refardt, D., Bergmiller, T. & Kümmerli, R. (2013). Altruism can evolve when relatedness is low: Evidence from bacteria committing suicide upon phage infection. *Proc. R. Soc. B Biol. Sci.*, 280, 20123035.

Reise, K., Olenin, S. & Thieltges, D.W. (2006). Are aliens threatening European aquatic coastal ecosystems? *Helgol. Mar. Res.*, 60, 77–83.

Rosenzweig, M.L. (1971). Paradox of enrichment: Destabilization of exploitation ecosystems in ecological time. *Science*, 171, 385–387.

Rosenzweig, M.L. & MacArthur, R.H. (1963). Graphical Representation and Stability Conditions of Predator-Prey Interactions. *Am. Nat.*, 97, 209–223.

Rossberg, A.G. (2013). *Food Webs and Biodiversity: Foundations, Models, Data.* Wiley.

Rossberg, A.G., Brännström, A. & Dieckmann, U. (2010). How trophic interaction strength depends on traits — A conceptual framework for representing multidimensional trophic niche spaces. *Theor. Ecol.*, 3, 13–24.

Rossberg, A.G., Farnsworth, K.D., Satoh, K. & Pinnegar, J.K. (2011). Universal power-law diet partitioning by marine fish and squid with surprising stability-diversity implications. *Proceeding R. Soc. B*, 278, 1617–1625.

Rossberg, A.G., Gaedke, U. & Kratina, P. (2019). Dome patterns in pelagic size spectra reveal strong trophic cascades. *Nat. Commun.*, 10, 1–11.

Rossberg, A.G., Houle, J.E. & Hyder, K. (2013). Stock-recruitment relations controlled by feeding interactions alone. *Can. J. Fish. Aquat. Sci.*, 70, 1447–1455.

Rossberg, A.G., Ishii, R., Amemiya, T. & Itoh, K. (2008). The top-down mechanism for body-mass–abundance scaling. *Ecology*, 89, 567–580.

Rossberg, A.G., Matsuda, H., Amemiya, T. & Itoh, K. (2006). Food webs: Experts consuming families of experts. *J. Theor. Biol.*, 241, 552–563.

Roy, S. & Chattopadhyay, J. (2007). The stability of ecosystems: A brief overview of the paradox of enrichment. *J. Biosci.*, 32, 421–428.

Ruokonen, T.J., Karjalainen, J. & Hämäläinen, H. (2014). Effects of an invasive crayfish on the littoral macroinvertebrates of large boreal lakes are habitat specific. *Freshw. Biol.*, 59, 12–25.

Sandström, A., Andersson, M., Asp, A., Bohman, P., Edsman, L., Engdahl, F., Nyström, P., Stenberg, M., Hertonsson, P., Vrålstad, T. & Granèli, W. (2014). Population collapses in introduced non-indigenous crayfish. *Biol. Invasions*, 16, 1961–1977.

Sanjuán, R., Moya, A. & Elena, S.F. (2004). The distribution of fitness effects caused by single-nucleotide substitutions in an RNA virus. *Proc. Natl. Acad. Sci. U. S. A.*, 101, 8396–8401.

Schaffer, W.M. & Rosenzweig, M.L. (1978). Homage to the Red Queen. I. Coevolution of predators and their victims. *Theor. Popul. Biol.*, 14, 135–157.

Schino, G. & Aureli, F. (2010). The relative roles of kinship and reciprocity in explaining primate altruism. *Ecol. Lett.*, 13, 45–50.

Schöps, K. (2002). Local and regional dynamics of a specialist herbivore: Overexploitation of a patchily distributed host plant. *Oecologia*, 2, 256–263.

Schreiber, S.J., Patel, S. & terHorst, C. (2018). Evolution as a Coexistence Mechanism: Does Genetic Architecture Matter? *Am. Nat.*, 191, 407–420.

Sheldon, R.W., Prakash, A. & Sutcliffe Jr., W.H. (1972). The size distribution of particles in the ocean. *Limnol. Oceanogr.*, 17, 327–340.

Shertzer, K.W. & Conn, P.B. (2012). Spawner-recruit relationships of demersal marine fishes: Prior distribution of steepness. *Bull. Mar. Sci.*, 88, 39–50.

Shiganova, T.A. (1998). Invasion of the Black Sea by the ctenophore *Mnemiopsis leidyi* and recent changes in pelagic community structure. *Fish. Oceanogr.*, 7, 305–310.

Shmida, A. & Wilson, M.V. (1985). Biological determinants of species diversity. *J. Biogeogr.*, 12, 1–20.

Silander, O.K., Tenaillon, O. & Chao, L. (2007). Understanding the evolutionary fate of finite populations: The dynamics of mutational effects. *PLoS Biol.*, 5, e94.

Simberloff, D. & Gibbons, L. (2004). Now you see them, now you don't! – population crashes of established introduced species. *Biol. Invasions*, 6, 161–172.

Skalski, G.T. & Gilliam, J.F. (2001). Functional responses with predator interference: Viable alternatives to the Holling type II model. *Ecology*, 82, 3083–3092.

Slatkin, M. & Maynard Smith, J. (1979). Models of coevolution. *Q. Rev. Biol.*, 54, 233–263.

Slobodkin, L.B. (1960). Ecological energy relationships at the population level. *Am. Nat.*, 94, 213–236.

Slobodkin, L.B. (1964). Experimental populations of Hydrida. *J. Anim. Ecol.*, 33, 131–148.

Slobodkin, L.B. (1974). Prudent predation does not require group selection. *Am. Nat.*, 108, 665–678.

Slobodkin, L.B. (2009). My complete works and more. *Evol. Ecol. Res.*, 11, 327–354.

Stouffer, D.B. & Novak, M. (2021). Hidden layers of density dependence in consumer feeding rates. *Ecol. Lett.*

Taylor, A.D. (1990). Metapopulations, dispersal, and predator-prey dynamics: An overview. *Ecology*, 71, 429–433.

Taylor, A.D. (1991). Studying metapopulation effects in predator-prey systems. *Biol. J. Linn. Soc. Lond.*, 42, 305–323.

Thorson, J.T., Dorn, M.W. & Hamel, O.S. (2019). Steepness for West Coast rockfishes: Results from a twelve-year experiment in iterative regional meta-analysis. *Fish. Res.*, 217, 11–20.

Tillberg, C.V., Holway, D.A., LeBrun, E.G. & Suarez, A.V. (2007). Trophic ecology of invasive Argentine ants in their native and introduced ranges. *Proc. Natl. Acad. Sci.*, 104, 20856–20861.

Tuljapurkar, S., Boe, C. & Wachter, K.W. (1994). Nonlinear feedback dynamics in fisheries: Analysis of the Deriso–Schnute model. *Can. J. Fish. Aquat. Sci.*, 51, 1462–1473.

Tyutyunov, Y.V. & Titova, L. (2020). From Lotka–Volterra to Arditi–Ginzburg: 90 years of evolving trophic functions. *Biol. Bull. Rev.*, 10, 167–185.

Uiterwaal, S.F., Lagerstrom, I.T., Lyon, S.R. & DeLong, J.P. (2018). Data paper: FoRAGE (Functional Responses from Around the Globe in all Ecosystems) database: A compilation of functional responses for consumers and parasitoids. *bioRxiv*, p. 503334.

van Leeuwen, E., Brännström, A., Jansen, V.A.A., Dieckmann, U. & Rossberg, A.G. (2013). A generalized functional response for predators that switch between multiple prey species. *J. Theor. Biol.*, 328, 89–98.

van Velzen, E. & Gaedke, U. (2017). Disentangling eco-evolutionary dynamics of predator-prey coevolution: The case of antiphase cycles. *Sci. Rep.*, 7, 17125.

Vetrano, S.J., Lebowitz, J.B. & Marcus, S. (2002). Lionfish envenomation. *J. Emerg. Med.*, 23, 379–382.

Yoccoz, N.G., Ellingsen, K.E. & Tveraa, T. (2018). Biodiversity may wax or wane depending on metrics or taxa. *Proc. Natl. Acad. Sci. U. S. A.*, 115, 1681.

Zhou, S., Yin, S., Thorson, J. & Fuller, M. (2012). Linking fishing mortality reference points to life history traits: An empirical study. *Can. J. Fish. Aquat. Sci.*, 69, 1292–1301.

Supporting Information
for
Evolution of prudent predation in complex food webs: mechanism and evidence

Orestes Uxio Gutierrez Al-Khudhairy and Axel G. Rossberg

May 26, 2021

Appendix S1 Motivation of our algorithm for sampling species

We explain here in detail why Eqs. (3) and (4) are plausible approximations for sampling the interaction strengths of new species entering our model community.

Under quite general conditions it is possible to approximate the dependence of attack rates on the traits of consumers and resources in the form (Rossberg *et al.*, 2010; Nagelkerke & Rossberg, 2014; Rossberg, 2013, Ch. 8):

$$a_{jk} \approx a_0 \exp\left[v_0^{(j)} + f_0^{(k)} - \sum_{k=1}^{D} \frac{\sigma_k}{2}\left(v_k^{(j)} - f_k^{(k)}\right)^2\right], \tag{S1}$$

with D denoting the dimensionality of trophic niche space and $v_0^{(j)}, \ldots, v_D^{(j)}$ and $f_0^{(k)}, \ldots, f_D^{(k)}$ *vulnerability-* and *foraging traits* of resources and consumers, respectively, which can be computed as functions of observable biological traits (Nagelkerke & Rossberg, 2014). A similar representation has been proposed by Rohr *et al.* (2010). The constant a_0 has dimensions of attack rates and $\sigma_k = \pm 1$. There is some ambiguity in how to chose a_0, σ_k and the functions mapping observed traits to trophic traits. However, when imposing a condition the mean of $(v_0^{(j)})^2$ over the entire resource pool j is minimised, these ambiguities are resolved up to rigid geometric transformations of the vectors $\mathbf{v}^{(j)} = (v_1^{(j)}, \ldots, v_D^{(j)})$ and $\mathbf{f}^{(k)} = (f_1^{(j)}, \ldots, f_D^{(j)})$ (Rossberg, 2013, Ch. 8). With the mean of $(v_0^{(j)})^2$ minimised, we shall approximate $v_0^{(j)} = 0$.

For large D and sufficient statistical independence of the components of $\mathbf{v}^{(j)}$ and $\mathbf{f}^{(k)}$ (Rossberg, 2013, Ch. 11), one can approximate the sum in Eq. (S1) for randomly sampled consumer-resource pairs (j, k) by a normal distribution. Denoting the mean of this normal distribution by μ and its variance by σ^2, and defining $a_k = a_0 \exp(f_0^{(k)} - \mu)$, this leads to Eq. (4).

All traits of consumers and resources can undergo mutations. However, compared to the evolution of foraging traits $f_0^{(k)}, \ldots, f_D^{(k)}$, the resulting evolution of vulnerability traits $v_0^{(j)}, \ldots, v_D^{(j)}$ is known to be slow (Rossberg *et al.*, 2006; Bersier & Kehrli, 2008; Eklöf & Stouffer, 2016)—a median of 25 times slower in an analysis of Rossberg *et al.* (2006). It shall here be disregarded.

Mutations of any observable biological traits will affect several foraging traits $f_0^{(k)}, \ldots, f_D^{(k)}$. The question whether this increases of decreases *short-term fitness* (Goodnight *et al.*, 2008) in a given community depends not only on all traits $f_0^{(k)}, \ldots, f_D^{(k)}$ of the focal consumer k but also on the sets of resources and competitors in the community. Even when a mutation leads to an increase in short-term

fitness, the change in $f_0^{(k)}$ associated with this mutation might be positive or negative, provided niche space dimensionality D is not too low, since the associated change in $f_0^{(k)}$ is just one of many random contributions to the change in short-term fitness. As a result, mutants arriving at the focal patch from a source patch may have $f_0^{(k)}$ values that can be higher or lower than the $f_0^{(k)}$ of the propagule that founded the population in the source patch. Because smaller $f_0^{(k)}$ correspond to consumers that, overall, forage less effectively than consumers with larger $f_0^{(k)}$, and low effectiveness is mechanically easier to achieve than high effectiveness, one must plausibly assume that degeneration of traits through mutations (Pomiankowski *et al.*, 1991) leads to a decay of $f_0^{(k)}$ on average unless this is counteracted by selection pressure. Recalling that $a_k = a_0 \exp(f_0^{(k)} - \mu)$, this leads to Eq. (3).

We assume that the relevant species pools are large and diverse, such that different patches have in effect statistically independent, typically non-overlapping species compositions. The random variables ξ_{jk} in Eq. (4) are therefore sampled anew as a propagule arrives at the focal patch, independent of a consumer's interactions with the residents of its source patch. Only the inheritance of a_k must be accounted of.

As a caveat, we note that in reality vulnerability traits do not cover the D-dimensional trophic traits space evenly, e.g. because these traits carry phylogenetic signal (related species have similar consumers, Bersier & Kehrli 2008). Then foraging traits other than $f_0^{(k)}$ might contribute to long-term fitness as well. For simplicity, we disregard this complication in our model.

Appendix S2 Derivation of the sub-models of the deconstructed formulation

We provide the rationale and outline the derivation of the four criteria Eqs. (5-9) driving invasions and extirpations in the deconstructed model formulation.

The *invadability criterion*, Eq. (5), predicts invadability when disregarding the presence of all but the focal consumer in the dimensionless full model, Eq. (2). Formally, it is obtained by computing the equilibrium state of Eq. (2) for $S_\mathrm{C} = 1$ and $B_k^\mathrm{C} = 0$ (with $k = 1$), which is $B_j^\mathrm{R} = 1$ for $1 \leq j \leq S_\mathrm{R}$, and then extracting the condition that, by Eq. (2b), this equilibrium is unstable such that the consumer can invade: $\sum_{j=1}^{S_\mathrm{R}} H_{jk} B_j^\mathrm{R} - 1 = \sum_{j=1}^{S_\mathrm{R}} H_{jk} - 1 > 0$.

The condition for the *overexploitation* of resource j during the expansion phase of an invading consumer k, Eq. (7), is obtained by analysing the dimensionless full model, Eq. (2), for the case of only one consumer and one resource: $S_\mathrm{C} = 1$, $S_\mathrm{R} = 1$ (with $j = k = 1$). We consider again the situation where the consumer is initially absent $B_k^\mathrm{C} = 0$ and the resource at equilibrium $B_j^\mathrm{R} = 1$, $dB_j^\mathrm{R}/dt = 0$. Then the consumer invades at low abundance. To estimate the minimum of B_j^R attained during the consumer invasion, i.e. during the transient before a new equilibrium is reached, we approximate dynamics by disregarding the density dependence of resource production expressed by the term $-B_j^\mathrm{R}$ in Eq. (2a). This approximation is justified because we are interested in situations where B_j^R falls below $M_\mathrm{min} \ll 1$. It reduces the model to the classical Lotka-Volterra predator-prey equations

$$\frac{dB_j^\mathrm{R}}{dt} = s \left[1 - H_{jk} B_k^\mathrm{C} \right] B_j^\mathrm{R}, \tag{S2a}$$

$$\frac{dB_k^\mathrm{C}}{dt} = \rho_k \left[H_{jk} B_j^\mathrm{R} - 1 \right] B_k^\mathrm{C}. \tag{S2b}$$

Evaluating the conservation law known for this system (Lotka, 1920) for the initial conditions $B_j^\mathrm{R} = 1$, $dB_j^\mathrm{R}/dt = 0$, one finds that at its minimum B_j^R satisfies $\ln(B_j^\mathrm{R}) = -H_{jk}(1 - B_j^\mathrm{R})$ (Rossberg, 2013, Sec. 20.3.3). Since we are interested in situations where the minimum is deep ($B_j^\mathrm{R} < M_\mathrm{min} \ll 1$), this condition can be approximated as $\ln(B_j^\mathrm{R}) = -H_{jk}$. It follows that B_j^R falls below M_min during consumer k's invasion if $\ln(M_\mathrm{min}) > -H_{jk}$, which is equivalent to Eq. (7).

The conditions for *consumer-mediated competitive exclusion*, for *exploitative competitive exclusion* and for *Pyrrhic competition* all derive directly from exact equilibrium solutions of the dynamic model. The general multispecies model, Eq. (2), is well studied (MacArthur, 1970, 1972; Case & Casten, 1979; Chesson, 1990). To write down its equilibrium solution, let $\mathbf{H}$ be the matrix with entries H_{jk} and define the competition matrix as the matrix with entries

$$C_{kl} = \sum_{j=1}^{S_\mathrm{R}} H_{jk} H_{jl}, \quad \text{that is} \quad \mathbf{C} = \mathbf{H}^T \mathbf{H}. \tag{S3}$$

Denote by $\mathbf{s}$ the vector of intrinsic consumer growth rates

$$s_k = R_k - 1, \tag{S4}$$

with $R_k = \sum_{j=1}^{S_\mathrm{R}} H_{jk}$ defined as in the main text. The vector $\mathbf{b}^\mathrm{C}$ of consumer population biomasses B_j^C at equilibrium is then given by

$$\mathbf{b}^\mathrm{C} = \mathbf{C}^{-1} \mathbf{s}. \tag{S5}$$

and that of resource population biomasses B_j^{R} by

$$\mathbf{b}^{\mathrm{R}} = 1 - \mathbf{H}\mathbf{B}^{\mathrm{C}}. \tag{S6}$$

In the case of only one consumer ($S_{\mathrm{C}} = 1$, $k = 1$), the biomass of the resource j is therefore $B_j^{\mathrm{R}} = 1 - H_{jk}(C_{kk})^{-1}s_k$. The resource with the lowest biomass is that with the largest H_{jk}, i.e., the main resource of k. Its biomass is negative, implying resource extinction (Holt, 1977), if

$$C_{kk} < H_{jk}s_k. \tag{S7}$$

The criterion for consumer-mediated competitive exclusion, Eq. (8), spells out this condition.

For the two-consumer ($S_c = 2$) problem, we have, with $k = 1$ and $l = 2$,

$$\mathbf{C}^{-1} = \frac{1}{C_{kk}C_{ll} - C_{kl}^2}\begin{pmatrix} C_{ll} & -C_{kl} \\ -C_{kl} & C_{kk} \end{pmatrix}. \tag{S8}$$

Combining Eqs. (S5) and (S8), we find that (for $S_c = 2$) $B_k^C < 0$ if

$$C_{ll}s_k - C_{kl}s_l < 0 \tag{S9}$$

or equivalently

$$s_k < \frac{C_{kl}s_l}{C_{ll}}. \tag{S10}$$

Our criterion of exploitative competitive exclusion, Eq. (6) spells out this condition.

Now, assume that Eq. (S10) and the corresponding condition with l's and k's role reversed both fail to be satisfied. This alone does not guarantee coexistence of all species. Combining Eqs. (S5), (S6) and (S8), one can see that the equilibrium abundance of resource B_i^{R} is predicted to be negative if

$$1 < H_{ik}\frac{C_{ll}s_k - C_{kl}s_l}{C_{kk}C_{ll} - C_{kl}^2} + H_{il}\frac{C_{kk}s_l - C_{kl}s_k}{C_{kk}C_{ll} - C_{kl}^2}. \tag{S11}$$

This can be re-arranged to

$$C_{kk}C_{ll} - C_{kl}^2 < s_k\left(H_{ik}C_{ll} - H_{il}C_{kl}\right) + s_l\left(H_{il}C_{kk} - H_{ik}C_{kl}\right), \tag{S12}$$

and our condition for Pyrrhic competition, Eq. (9), spells out this inequality.

We now outline how these conditions can efficiently be evaluated for large S_{R} and S_{C}. The most time consuming step is the computation of $\mathbf{C}$ in Eq. (S3), as (for practical purposes) the number of operations this requires increases as $\mathcal{O}(S_{\mathrm{C}}^2 S_{\mathrm{R}})$ with system size. All remaining calculations can be done using just $\mathcal{O}(S_{\mathrm{C}}^2)$ or $\mathcal{O}(S_{\mathrm{C}}S_{\mathrm{R}})$ operations.

Denote, for any square matrix A, by $\mathbf{diag}(A)$ the vector formed by its diagonal elements, and by $\mathbf{Diag}(\mathbf{v})$, for any vector $\mathbf{v}$, the diagonal matrix with $\mathbf{v}$ on the diagonal. We can evaluate the $S_{\mathrm{C}} \times S_{\mathrm{C}}$ matrix $\mathbf{\Phi}$ with entries Φ_{kl} given by the left hand side of Eq. (S9) as

$$\mathbf{\Phi} = \mathbf{s}\,\mathbf{diag}(\mathbf{C})^T - \mathbf{C}\,\mathbf{Diag}(\mathbf{s}). \tag{S13}$$

To test for extirpations, set the diagonal of $\mathbf{\Phi}$ to exactly zero to remove small numerical errors. Extirpation of consumer k by our (simplified) criterion follows if row k of $\mathbf{\Phi}$ constrains negative elements.

The $S_C \times S_C$ matrix $\mathbf{D}$ with entries $D_{kl} = C_{kk}C_{ll} - C_{kl}^2$, containing the determinants of all two-consumer competition problems (the denominators in Eqs. (S8), (S11)), can be computed as

$$\mathbf{D} = \mathbf{diag}(\mathbf{C})\,\mathbf{diag}(\mathbf{C})^T - \mathbf{C} \circ \mathbf{C}, \tag{S14}$$

with $\circ$ denoting elementwise multiplication. After finding for each consumer k the index $m(k)$ of its main resource, one can constructed the $S_C \times S_C$ matrix $\mathbf{M}$ with entries

$$M_{kl} = H_{m(k)l}. \tag{S15}$$

Using this, we obtain the $S_C \times S_C$ matrix $\mathbf{\Delta}$ with entries given by the difference between left and right hand side of Eq. (S12) for the main resource of each consumer k as

$$\mathbf{\Delta} = \mathbf{D} - \mathbf{Diag}(\mathbf{diag}(\mathbf{M}))\mathbf{\Phi} - \mathbf{M} \circ \mathbf{\Phi}^T. \tag{S16}$$

To test for extirpations, set the diagonal of $\mathbf{\Delta}$ to exactly zero to remove small numerical errors. Extirpation of the main resource of consumer k by our (simplified) criterion follows if row k of $\mathbf{\Delta}$ contains negative elements.

By striking a new balance between code complexity, speed, and accuracy in the multi-objective optimisation problem of finding fast, simple and accurate models, our deconstructed formulation carves out emergent properties (*sensu* Rossberg, 2007) of the full model, Eq. (2), e.g., those shown in Figs. 2 and 3.

Appendix S3 The evolutionary steady-state condition including mutation bias

We derive the evolutionary steady state condition for base attack rate, Eq. (11).

To understand the effect of mutation bias, we invoke the Price equation (Price, 1972). It predicts that the expected rate of evolutionary change of the a trait q is given by

$$d\mathsf{E}q/dt = \mathrm{cov}[f(q), q] + \mathsf{E}\dot{q}, \tag{S17}$$

with $f(q)$ denoting the invasion fitness (for a given environment) of lineages of type q, and the last term representing the mutation bias (the mean inherent rate of change of traits). For trait values q^* corresponding to evolutionary steady states, both sides of Eq. (S17) must evaluate to zero. Following Page & Nowak (2002), we expand $f(q)$ to first order at $q = q^*$. Combined with the population-dynamical equilibrium condition $f(q^*) = 0$, this leads to $0 = f'(q^*)\,\mathrm{var}\,q + \mathsf{E}\dot{q}$, or equivalently

$$f'(q^*) = -\frac{\mathsf{E}\dot{q}}{\mathrm{var}\,q}. \tag{S18}$$

This condition generalises the conventional criterion for evolutionary singular strategies, $f'(q^*) = 0$, to situations with mutation bias.

To apply Eq. (S18) to our models, we set $q = \ln a$ and

$$\mathsf{E}\dot{q} = \frac{\ln \gamma_0}{L^*}, \tag{S19}$$

where L^* is the mean lifetime of populations in the community. With time measured in units of consumer additions and considering that consumer richness remains approximately constant in the steady state, $L^* = S_\mathrm{C}^{-1}$. The standing mutational variance $\mathrm{var}\,q = \mathrm{var}(\ln a)$ is obtained from the distribution of a over the simulation steady state.

We approximate steady-state invasion fitness, i.e. the mean inherent rate of increase ($f(q) > 0$) or decrease ($f(q) < 0$) of the number of populations of type q in the simulation steady state, as $f(q) \approx \ln[R(a)]/L(a)$, where $R(a)$ is the mean number of populations that inherit their base attack rate *via* Eq. (3) from a population with base attack rate a (the "mean lifetime reproductive success"), and $L(a)$ is the mean lifetime of populations with base attack rate a. With a^* representing the geometric mean of a over the simulation steady state, such that $\ln a^*$ is the arithmetic mean of $\ln a$, we expect that $R(a^*) = 1$. This leads to

$$f'(q^*) \approx \left.\frac{d\{\ln[R(a)]/L(a)\}}{d\ln a}\right|_{a=a^*} = \left.\frac{1}{L(a)}\frac{d\ln[R(a)]}{d\ln a}\right|_{a=a^*} \approx \left.\frac{1}{L^*}\frac{d\ln[R(a)]}{d\ln a}\right|_{a=a^*}. \tag{S20}$$

Putting Eqs. (S19) and (S20) into Eq. (S18) and multiplying both sides with L^* yields Eq. (11).

Appendix S4 Mechanisms determining "birth rate"

To derive an analytic representation of the dependence of birth rate $b(a)$ of a resident consumer on base attack rate a, we must account for three elements common to both model formulations:

1. The mutation step, Eq. (3), determining the new consumer's based attack rate from that of the resident.

2. The sampling of the new consumer's attack rates according to Eq. (4), and the test whether it can invade.

3. The fact that time is measured in numbers of successful consumer invasions.

Crucial is the probability of successful invasion in 2. We begin with an analysis of this element, adding subsequently considerations of 1 and 3.

Competitive exclusion by a resident consumer according to Eq. (6) always implies an inability to invade according to Eq. (5), so that (for $S_\mathrm{C} > 0$) only Eq. (6) needs to be considered. However, Eq. (5) can be understood as a correction of the invadability criterion, Eq. (5). To see this, re-arrange Eq. (6) as

$$\sum_{j=1}^{S_\mathrm{R}} H_{jk} \left[1 - H_{jl} \frac{\sum_{i=1}^{S_\mathrm{R}} H_{il} - 1}{\sum_{i=1}^{S_\mathrm{R}} H_{il}^2} \right] - 1 < 0. \tag{S21}$$

The term in square brackets represents the population biomass (in units of K) that resource j would have if l was the only extant consumer. The deconstructed formulation ensures that, at the end of a model iteration, no extant resource satisfies the criterion for consumer-mediated competitive exclusion, Eq. (8) and all extant consumers satisfy the simple invadability criterion, Eq. (5). These loop invariants guarantees that the value of the expression in brackets in Eq. (S21) lies between 0 and 1 for all k and l. Satisfaction of Eq. (S21) therefore implies violation of Eq. (5).

Because there is no mechanism active in the model that would favours values of the expression in square brackets that are particularly close to zero (see also Fig. S1), most of the variation in the terms of the sum over j is due to the log-normal distribution of the invader's attack rates H_{jk}. The presence of competitors merely moderates the effect of this variation. It can be represented by substituting the square bracket by a suitable constant $0 < \beta < 1$: the fitting parameter introduced in the main text.

The sum over j in Eq. (S21) can then be written as $\alpha_0 a_k \beta \sum_{j=1}^{S_\mathrm{R}} e^{\sigma \xi_{jk}}$. The distribution of the sum in this last expression is, for a given number of resources S_R, often well approximated by a single log-normal distribution with suitable choices for mean $\mu_{S_\mathrm{R}} \approx \sigma\sqrt{2 \ln S_\mathrm{R}}$ and standard deviation $\sigma_{S_\mathrm{R}} \approx \sigma/\sqrt{1 + 2 \ln S_\mathrm{R}}$ of the logarithm (Rossberg *et al.*, 2011). (We estimated μ_{S_R} and σ_{S_R} numerically form 10,000 samples of log-normal sums, which is more accurate.)

From this log-normal approximation, the invasion probability for species with given base attack rate a_k is obtained as

$$P_\mathrm{inv}(a_k) = \Phi\left(\frac{\ln(\alpha_0 \beta a_k) + \mu_{S_\mathrm{R}}}{\sigma_{S_\mathrm{R}}} \right), \tag{S22}$$

with $\Phi(x)$ denoting the cumulative standard normal distribution function. For the full model, the same functional form as in Eq. (S22) can be chosen based on the same rationale: compared to the variation in of link strengths, the variation in resource biomasses is small.

Denote by $P^*_\mathrm{inv}(a_r)$ the probability for the "offspring" of resident species r to invade successfully. The log-normal approximation for the sum in $\alpha_0 a_k \beta \sum_{j=1}^{S_\mathrm{R}} e^{\sigma \xi_{jk}}$ used above combines seamlessly with the log-normal distribution of a_k resulting from the mutation of base attack rate a_r of the resident "parent"

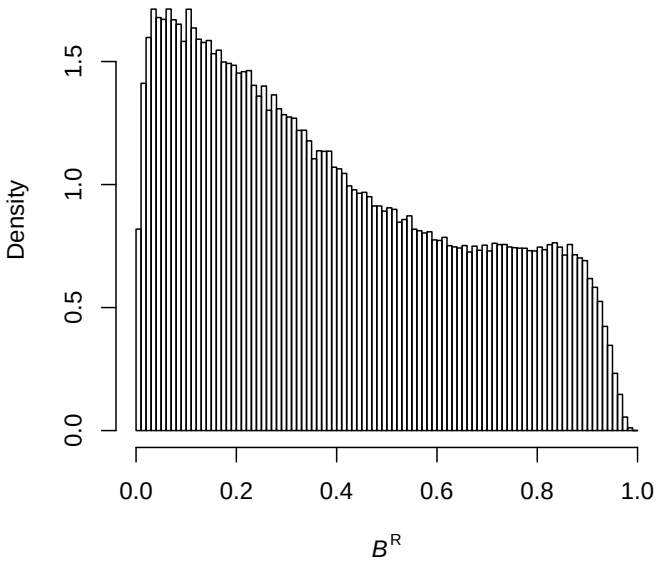

Figure S1: Histogram of resource biomasses B^{R} in the steady state of the full model, sampled from community snapshots after every 200 consumer additions. Neither values close to zero nor values close to one are very frequent.

species as per Eq. (3). We can therefore obtained $P^*_{\mathrm{inv}}(a_r)$ from Eq. (S22) by correcting $\mu^*_{S_{\mathrm{R}}} = \mu_{S_{\mathrm{R}}} + \ln\gamma_0$ and $\sigma^*_{S_{\mathrm{R}}} = [\sigma^2_{S_{\mathrm{R}}} + (\ln\gamma_1)^2]^{1/2}$ to account for mutational variance and bias. Hence

$$P^*_{\mathrm{inv}}(a_r) = \Phi\left(\frac{\ln(\alpha_0\beta a_r) + \mu^*_{S_{\mathrm{R}}}}{\sigma^*_{S_{\mathrm{R}}}}\right). \tag{S23}$$

Because we measure time in units of consumer invasions, and both variants of our model attempt consumer invasions from random resident species until one succeeds, the probability for offspring of resident consumer r to invade in a given time step is $P^*_{\mathrm{inv}}(a_r)/\sum_{k=1}^{S_{\mathrm{C}}} P^*_{\mathrm{inv}}(a_k)$ (guaranteeing that the probability for offspring of some consumer k to invade evaluates to 1). Since species richness and the distribution of a_r fluctuate somewhat through time, we calculated the "birth" rate in Fig. 3c,g as the average of this probability for a given base attack rate a over the model steady states:

$$b(a) = \text{Average through time of } \frac{P^*_{\mathrm{inv}}(a)}{\sum_{k=1}^{S_{\mathrm{C}}} P^*_{\mathrm{inv}}(a_k)}. \tag{S24}$$

Appendix S5 Serial extinction

We derive Eq. (15) for the consumer's intrinsic growth rate after serial extinction

Note first that, because resources are successively removed in decreasing order of the consumer's attack rate in the deconstructed model formulation (and also in the simplified model, Box 2), the distribution of attack rates after serial extinction is the same as before, except for being truncated from above at the point where Eq. (8) becomes violated. In situations where the sums in Eq. (8) are not dominated by just a few resources, the central limit theorem can be invoked and the sums approximated by their expectation values, which then permits analytic computation of the truncation threshold H_* and other properties of the end state.

The calculations simplify by first approximating the relevant section of the upper tail of the log-normal attack-rate distribution, Eq. (4), by a Pareto distribution, which can be derived in the limit of high resource richness S_R (Rossberg *et al.*, 2011; Rossberg, 2013). By this approximation, the consumer has on average Z resources with H_{jk} larger then some "observation threshold" H_0, and for these

$$P[H_{jk} \leq x] \approx 1 - \left(\frac{H_0}{x}\right)^\nu, \tag{S25}$$

with $\nu = \sigma^{-1}\sqrt{2\ln S_\mathrm{R}}$. Empirically, typical values for ν are in the range 0.5 to 0.6 (Rossberg *et al.*, 2011; Rossberg, 2013). Values $\nu \geq 1$ would correspond to extreme omnivory where the proportional contribution of each resource species to a consumer's diet scales as $1/S_\mathrm{R}$, i.e. no resource makes a sizeable contribution to the diet. We are unaware of such a situation occurring in nature, and therefore assume $0 < \nu < 1$ in this study. The value of the link density Z is chosen to control the typical strengths H_max of the strongest attack rate before serial extinction, specifically the $\exp(-1)$-quantile of the distribution of $\max_j H_{jk}$. In the limit of large Z, this leads to the condition

$$\exp(-1) = \left(P[H_{jk} \leq H_\mathrm{max}]\right)^Z = \left[1 - \left(\frac{H_0}{H_\mathrm{max}}\right)^\nu\right]^Z \approx \exp\left[-\left(\frac{H_0}{H_\mathrm{max}}\right)^\nu Z\right] \tag{S26}$$

and so

$$Z \approx \left(\frac{H_\mathrm{max}}{H_0}\right)^\nu. \tag{S27}$$

It goes without saying that H_max is proportional to base attack rate a_k and can therefore be use as a proxy for the latter.

With this preparation, we can now take expectation values on both sides of Eq. (8) for the case of truncation at H_*, the largest threshold where it is not violated, to approximate

$$\mathsf{E}\left[\sum_j^{H_{jk}\leq H_*} H_{jk} - 1\right] = H_*^{-1}\mathsf{E}\left[\sum_j^{H_{jk}\leq H_*} H_{jk}^2\right] \tag{S28}$$

as

$$\left[Z\int_{H_0}^{H_*} p(x)x\,dx - 1\right] = H_*^{-1} Z\int_{H_0}^{H_*} p(x)x^2\,dx, \tag{S29}$$

where $p(x) = -(d/dx)P[H_{jk} \leq x]$ is the probability density of the untruncated attack rate distribution. Evaluation of the integrals after inserting Eq. (S25) leads to

$$\frac{Z\nu H_*^{-\nu}\left(H_* H_0^\nu - H_*^\nu H_0\right)}{1-\nu} - 1 = H_*^{-1}\frac{Z\nu H_*^{-\nu}\left(H_*^2 H_0^\nu - H_*^\nu H_0^2\right)}{2-\nu} \tag{S30}$$

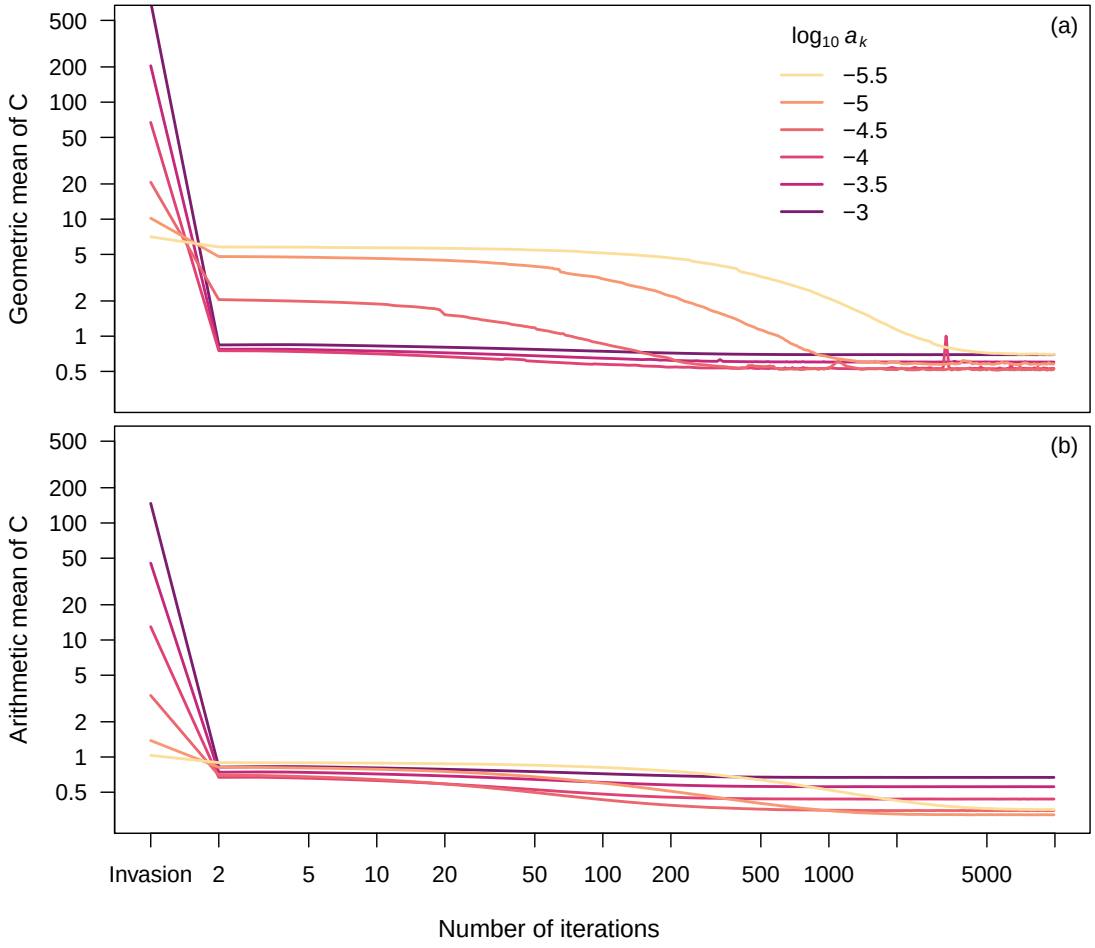

Figure S2: **Dependence of intrinsic growth rate** $\mathsf{C} = 1 - \sum_j H_{jk}$ **on base attack rate in the course of repeated serial extinction and resource turnover.** Panel (a) shows geometric means of C over 10^6 replicated runs of the model of Box 2 over 10^4 iterations, panel (b) arithmetic means. For high base attack rates a_k (dark lines), both geometric and arithmetic means approach the same value ≈ 0.86 (indicating a near-deterministic outcome) after the first iteration of consumer-mediated competitive exclusion, largely independent of base attack rate, as predicted by the analytic theory. The value is different from the analytic prediction $1 - \sigma^{-1}\sqrt{2 \log S_\mathsf{R}} \approx 0.14$ valid for large because S_R, because $S_\mathsf{R} = 224$ is not sufficiently large.

and, after inserting Eq. (S27) and taking the limit of low observation threshold ($H_0 \to 0$),

$$\frac{H_*^{-\nu}\left[\nu H_* H_{\max}^{\nu} - H_*^{\nu}(1-\nu)\right]}{1-\nu} = \frac{\nu H_*^{1-\nu} H_{\max}^{\nu}}{2-\nu}. \tag{S31}$$

This equation can be solved for H_*, yielding

$$H_* = \left[\frac{(1-\nu)(2-\nu)}{\nu H_{\max}^{\nu}}\right]^{1/(1-\nu)}. \tag{S32}$$

The expected intrinsic growth rate of the consumer after serial extinction equals the left hand sides of Eqs. (S28)-(S31). When putting Eq. (S32) into the left hand side of Eq. (S31) it simplifies considerably, leading to the final result

$$\mathsf{E}\left[\sum_k^{H_{ki} \le H_*} H_{ki} - 1\right] = 1 - \nu. \tag{S33}$$

With $0 < \nu < 1$, this result implies that $\mathsf{E}\sum_j^{H_{jk}\leq H_*} H_{jk}$ attains values between 1 and 2. On the other hand, the upper cutoff H_* declines with increasing $H_{\max}$ (or base attack rates a_i) as $H_{\max}^{-\nu/(1-\nu)}$ by Eq. (S32). For large base attack rates the sum $\sum_j^{H_{jk}\leq H_*} H_{jk}$ therefore has contributions from many small terms, justifying our application of the central limit theorem to approximate of the sums entering Eq. (8) by their expectation values. Figure S2b qualitatively confirms this result.

Interestingly, above considerations imply that, despite having the same niche width in terms of the spread σ of the log-normal attack-rate distribution, invaders with higher base attack rate will have more diverse diets post Impact than those with lower attack rates. This might explain why invasive alien consumers are often found to be 'generalists'.

Box 1 Algorithm of the evolutionary metapopulation model.

The model state is given by N patches which are either empty of occupied by a population with base attack rate a_i ($1 \leq i \leq N$). The model is simulated as follows:

1. Occupy a proportion p of patches with populations with identical initial base attack rates a_i.
2. Select an occupied source patch r for dispersal. Sample the base attack rate a_k of a propagule according to Eq. (3).
3. Sample a target patch l.
4. If patch l is occupied:
   (a) If $a_l < a_k$, replace the new population of patch l with one that has base attack rate a_k, otherwise do nothing.
5. If patch l is not occupied:
   (a) With invasion probability $P_{\text{inv}}(a_k)$, establish in patch l a new population with base attack rates a_k and then remove the population from another occupied patch m, sampled at random from all occupied patches with probability proportional to $1/L(a_m)$. $P_{\text{inv}}(a)$ is our approximation of invasion probability for the deconstructed community model, Eq. (S22) with $\beta = 0.45$ and $S_{\text{R}} = 224$ (corresponding to the mean equilibrium richness in Fig. 2), and $L(a)$ the polynomial fit to mean population life time in Fig. 3h ($\log_{10} L = -0.04105026(\log_{10} a)^2 - 0.78404937 \log_{10} a - 0.77341520$).
6. Continue from Step 2 for a predetermined number of interactions.

The values of γ_0, γ_1, and σ are as in Tab. 1.

The algorithm can be reformulated in such a way that only the list of a_i value of occupied patches i is kept in memory. In each iteration, Step 3a is then executed with probability p and otherwise Step 4a. When invasion is successful in Step 4a, the new a_k value is stored in the memory location where a_m was previously stored. This formulation permits us to take the limit $p \to 0$ while keeping the number of occupied patches pN fixed.

Appendix S6 The limited impact of cheaters

Cheaters exploit benefits offered by more altruistic conspecifics to their advantage, thus potentially counteracting the evolution of altruism. To obtain a bound on the impact of cheaters on prudent predation, we devised a simple evolutionary metapopulation model. The model describes a landscape of N patches that are either occupied by the focal species or not. The population occupying patch i has an associated base attack rate a_i.

In our metapopulation model we assume that cheating occurs if a population of the focal species disperses to a patch that is already occupied, and the propagule's base attack rate is larger than that of the resident in that patch. The propagule then replaces the resident population. This model disregards that conspecific propagules will not only differ in their base attack rates from residents, but also in other foraging traits (Appendix Appendix S1), and therefore have, on average, a reduced likelihood of establishment success. Our metapopulation model is therefore biased to overestimates the likelihood of cheating. We shall see that the predicted impact of cheating remains limited despite this.

Contrasting conventional stochastic patch occupancy models in the tradition of Levins (1969), patch occupancy p, i.e., the proportion of occupied patches, is a parameter in our model. The reason is evidence that species richness both at patch level (α) and at landscape level (γ) is regulated through ecological structural stability limits (O'Sullivan *et al.*, 2019), which our metapopulation model cannot explicitly represent. Mean occupancy is uniquely determined by α and γ as $p = \alpha/\gamma$. By fixing p we represent these limits implicitly.

The model is detailed in Box 1. We chose $pN = 1000$ over a range of p values, evaluated the algorithm over $4 \cdot 10^7$ iterations, and sampled base attack rates from the last 3/4 of each run to characterise the steady state (which was reached after less then a 10^{th} of iterations).

In the limit $p \to 0$, where cheating does not occur, the model attained a steady state with mean logarithmic base attack rate $\overline{\log_{10} a} = -5.14$, close to the value obtained with the deconstructed model, and an approximately normal distribution of $\log_{10} a$ in the steady state similar to that in Fig. 3e. These results further confirm our reconstruction of the fitness landscape in Fig. 3.

As shown in Fig. S3, $\overline{\log_{10} a}$ increases linearly with p for low p. An occupancy of $p = 0.3$, for example, leads to an approximate 3-fold increase in geometric mean base attack rates. Hence, cheating makes consumers somewhat less prudent, but does not fundamentally undermine the evolution of prudent predation.

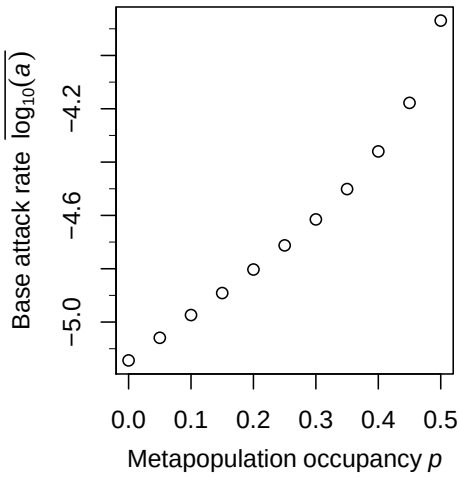

Figure S3: **The impact of cheaters on evolutionary stable base attack rate a.** Simulation results from the meta-population model described in Box 1. The higher the occupancy p of patches by the metapopulation, the larger the probability that occupied patches are overtaken by invading cheaters with higher base attack rates. This effect increases steady state base attack rates, but does not prevent a steady state from being reached.

Appendix S7 Steepness and basic reproduction number

We derive the relation between basic reproduction number and the steepness of stock recruitment relations given in Eq. (17).

Consider first the following caricature model of a fish stock feeding on a single resource:

$$\frac{dB^{\mathrm{R}}}{dt} = \left[s\left(1 - \frac{B^{\mathrm{R}}}{K}\right) - a\,\mathrm{SSB} \right] B^{\mathrm{R}}, \tag{S34a}$$

$$\frac{d\,\mathrm{SSB}}{dt} = \epsilon a B^{\mathrm{R}} \mathrm{SSB} - \rho\,\mathrm{SSB} - F\,\mathrm{SSB}. \tag{S34b}$$

The parameter F denotes the fishing mortality rate, otherwise model structure and parameterization are as in Eq. (1). If one assumes, for simplicity, that (i) all mature individuals have the same body mass m, (ii) recruits are produced instantaneously, and (iii) the parameter ρ is dominated by natural mortality rather than respiration, then recruitment is given by the first term on the right-hand side of Eq. (S34b):

$$m\,\mathrm{Rec} = \epsilon a B^{\mathrm{R}} \mathrm{SSB} = \epsilon a K\,\mathrm{SSB} - \frac{\epsilon a^2 K}{s} \mathrm{SSB}^2. \tag{S35}$$

In the second step we eliminated B^{R} by solving Eq. (S34a) with $dB^{\mathrm{R}}/dt = 0$ for $B^{\mathrm{R}} > 0$. Stock-recruitment relations of this quadratic form are frequently used in fisheries science and named after Schaefer (1954). Virgin ($F = 0$) equilibrium SSB evaluates to

$$\mathrm{SSB}_0 = s\frac{\epsilon a K - \rho}{\epsilon a^2 K}. \tag{S36}$$

From Eqs. (16), (S35) and (S36) one obtains the steepness

$$h = \frac{1}{25}\left(1 + \frac{4\epsilon a K}{\rho}\right). \tag{S37}$$

The basic reproduction number R is defined as recruitment per mature individual (of which there are SSB/m) in units of ρ, in the limit $\mathrm{SSB} \to 0$, which evaluates to

$$R = \lim_{\mathrm{SSB}\to 0} \frac{m\mathrm{Rec}}{\mathrm{SSB}\,\rho} = \frac{\epsilon a K}{\rho}. \tag{S38}$$

Hence Eq. (S37) implies Eq. (17).

We now verify that Eq. (17) remains valid if one generalises Eq. (S34) to a situation with multiple resources. We assume that the fish stock is initially fully established at SSB_0, such that resources that would not withstand its consumption have been extirpated. By Eq. (S6), the biomass of each resource is then a linear function of consumer biomass, here SSB. With the linear functional response of Lotka-Volterra models, this implies

$$m\,\mathrm{Rec} = (c_1 - c_2\,\mathrm{SSB})\,\mathrm{SSB} \tag{S39}$$

with some positive constants c_1 and c_2. As above, we can evaluate

$$R = \lim_{\mathrm{SSB}\to 0} \frac{m\mathrm{Rec}}{\mathrm{SSB}\,\rho} = \frac{c_1}{\rho}, \tag{S40}$$

yielding $c_1 = \rho R$. Furthermore, recruitment balances mortality for the unfish stocks with $\mathrm{SSB} = \mathrm{SSB}_0$. So $m\,\mathrm{Rec}(\mathrm{SSB}_0) = \rho\,\mathrm{SSB}_0$, which implies

$$c_2 = \rho \frac{R-1}{\mathrm{SSB}_0}. \tag{S41}$$

With these values for c_1, c_2, plugging Eq. (S39) into the definition of steepness, Eq. (16), yields again Eq. (17).

Supporting figures

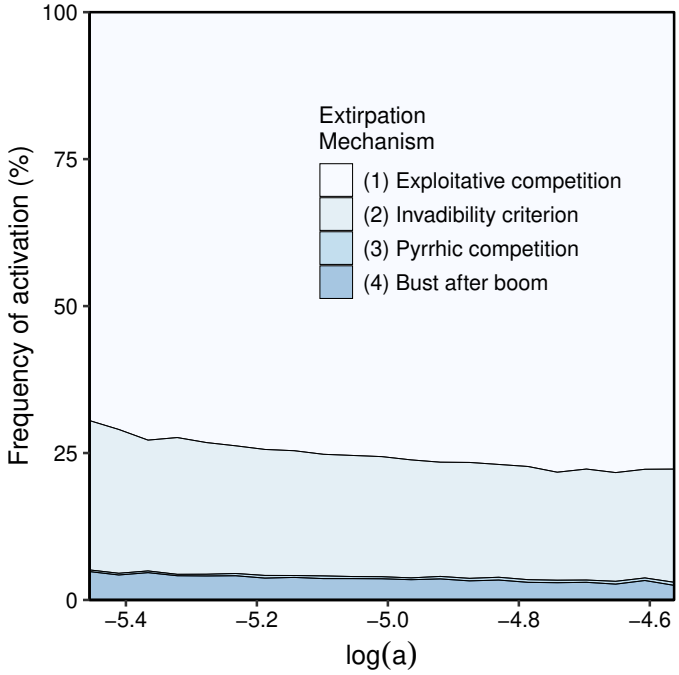

Figure S4: **Activation frequency of consumer extirpation mechanisms** The classification relates to different steps in the deconstructed model formulation (Box 1). *Exploitative competition* refers to Step 5; *Pyrrhic competition* to failure to meet the invadability condition by a consumer losing its main resource, or by the competitor causing this, in Steps 6, 7; *Bust after boom* refers to Step 3d; and *Invadability criterion* to failure to satisfy Eq. (5) at any other point in the algorithm. Extirpations through Pyrrhic competition are very rare, and those through bust after boom contribute just a few percent of cases.

References

Bersier, L.F. & Kehrli, P. (2008). The signature of phylogenetic constraints on food-web structure. *Ecol. Complex.*, 5, 132–139.

Case, T.J. & Casten, R.G. (1979). Global stability and multiple domains of attraction in ecological systems. *Am. Nat.*, 5, 705–714.

Chesson, P. (1990). MacArthur's consumer-resource model. *Theor. Popul. Biol.*, 37, 26–38.

Eklöf, A. & Stouffer, D.B. (2016). The phylogenetic component of food web structure and intervality. *Theor. Ecol.*, 9, 107–115.

Goodnight, C., Rauch, E., Sayama, H., de Aguiar, M.A.M., Baranger, M. & Bar-Yam, Y. (2008). Evolution in spatial predator-prey models and the "prudent predator": The inadequacy of steady-state organism fitness and the concept of individual and group selection. *Complexity*, 13, 23–44.

Holt, R.D. (1977). Predation, apparent competition, and the structure of prey communities. *Theor. Popul. Biol.*, 12, 197–229.

Levins, R. (1969). Some Demographic and Genetic Consequences of Environmental Heterogeneity for Biological Control. *Bull. Entomol. Soc. Am.*, 15, 237–240.

Lotka, A.J. (1920). Undamped oscillations derived from the law of mass action. *J. Am. Chem. Soc.*, 42, 1595–1599.

MacArthur, R. (1970). Species packing and competitive equilibrium for many species. *Theor. Popul. Biol.*, 1, 1–11.

MacArthur, R.H. (1972). *Geographical Ecology.* Harper and Row, New York.

Nagelkerke, L.A.J. & Rossberg, A.G. (2014). Trophic niche-space imaging, using resource and consumer traits. *Theor. Ecol.*, 7, 423–434.

O'Sullivan, J.D., Knell, R.J. & Rossberg, A.G. (2019). Metacommunity-scale biodiversity regulation and the self-organised emergence of macroecological patterns. *Ecol. Lett.*, 22, 1428–1438.

Page, K.M. & Nowak, M.A. (2002). Unifying Evolutionary Dynamics. *J. Theor. Biol.*, 219, 93–98.

Pomiankowski, A., Iwasa, Y. & Nee, S. (1991). The evolution of costly mate preferences I. Fisher and biased mutation. *Evolution*, 45, 1422–1430.

Price, G.R. (1972). Extension of covariance selection mathematics. *Ann. Hum. Genet.*, 35, 485–490.

Rohr, R.P., Scherer, H., Kehrli, P., Mazza, C. & Bersier, L.F. (2010). Modeling food webs: Exploring unexplained structure using latent traits. *Am. Nat.*, 176, 170–177.

Rossberg, A.G. (2007). Some first principles of complex systems theory. *RIMS Kôkyûroku*, 1551, 129–136.

Rossberg, A.G. (2013). *Food Webs and Biodiversity: Foundations, Models, Data.* Wiley.

Rossberg, A.G., Brännström, A. & Dieckmann, U. (2010). How trophic interaction strength depends on traits — A conceptual framework for representing multidimensional trophic niche spaces. *Theor. Ecol.*, 3, 13–24.

Rossberg, A.G., Farnsworth, K.D., Satoh, K. & Pinnegar, J.K. (2011). Universal power-law diet partitioning by marine fish and squid with surprising stability-diversity implications. *Proceeding R. Soc. B*, 278, 1617–1625.

Rossberg, A.G., Matsuda, H., Amemiya, T. & Itoh, K. (2006). Food webs: Experts consuming families of experts. *J. Theor. Biol.*, 241, 552–563.

Schaefer, M.B. (1954). Fisheries dynamics and the concept of maximum equilibrium catch. In: *Proceedings of the Gulf and Caribbean Fisheries Institute - 6th Annual Session.* pp. 53–64.